Self-Assembly

Grid-Type Metal Ion Architectures: Functional Metallosupramolecular Arrays

*Mario Ruben, Javier Rojo, Francisco J. Romero-Salguero, Lindsay H. Uppadine, and Jean-Marie Lehn**

Keywords:
coordination chemistry · molecular informatics · self-assembly · supramolecular chemistry · transition metals

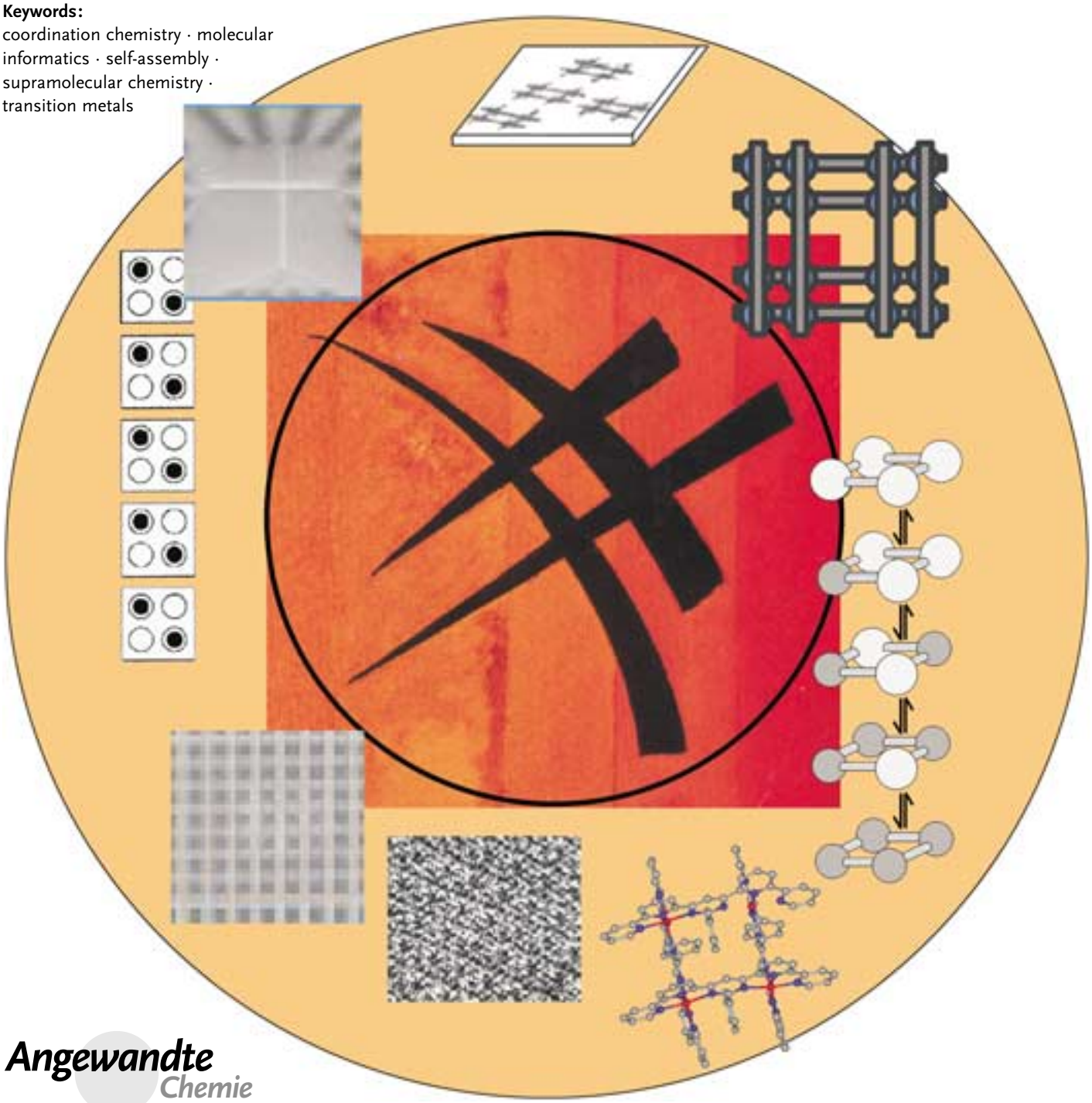

  DOI: 10.1002/anie.200300636

Recent advances in supramolecular coordination chemistry allow access to transition-metal complexes of grid-type architecture comprising two-dimensional arrays of metal ions connecting a set of organic ligands in a perpendicular arrangement to generate a multiple wiring network. General design principles for these structures involve the thermodynamically driven synthesis of complex discrete objects from numerous molecular components in a single overall operation. Such supramolecular metal ion arrays combine the properties of their constituent metal ions and ligands, showing unique optical, electrochemical, and magnetic behavior. These features present potential relevance for nanotechnology, particularly in the area of supramolecular devices for information storage and processing. Thus, a dense organization of addressable units is represented by an extended "grid-of-grids" arrangement, formed by interaction of grid-type arrays with solid surfaces.

From the Contents

1. Introduction	3645
2. General Concepts	3647
3. Grid-Type Metal Ion Arrays	3649
4. Mechanistic Features of the Self-Assembly Process	3654
5. Multistability and Addressability	3655
6. Conclusion and Outlook	3660

1. Introduction

The drive to shrink electronic devices to the nano-level, has, in recent years, led to the design and investigation of molecular-scale components endowed with sensing, switching, logic, and information storage functions.[1–3] Although the implementation of information processing with such devices faces hurdles in the development of logic architecture and intermolecular hook-up schemes,[1] molecular data storage is subject to active interest, namely in view of the rapidly approaching upper limit in conventional magnetic data storage resulting from thermal erasure at the superparamagnetic limit. Species suitable for molecular data storage must 1) possess two or more physicochemically distinct states that can be conveniently switched by application of external triggers (e.g. thermodynamic parameters or electromagnetic fields) and 2) should be addressable and switchable within the nanometer regime. Toward this end, gridlike metal ion arrays, in which a set of metal ions is held in a regular network of organic ligands in a perpendicular arrangement (Figure 1), present several attractive features: 1) their redox, magnetic, and spin-state transitions are well-documented, 2) the well-defined two-dimensional (2D) arrangement of an exact number of metal ions resembles strongly the binary coded matrices and cross-bar architectures used in information storage and processing technology, and 3) they may be arranged into extended two-dimensional ensembles by deposition onto solid surfaces. The nuclearity and dimensionality of the gridlike metalloarrays are clearly based on the polytopic nature of the ligands and the ability of the metal to read and interpret the coordination options presented by the ligand in the most efficient way depending on its own coordination algorithm.

Figure 1. Molecular structures of several gridlike metal ion arrays that exhibit a regular network of perpendicular arranged organic ligands.[4a, 5a, 6]

The two-dimensional (2D) grid motif was recently the architectural base of a molecular 64-bit logic and storage device.[7a] The resulting architecture consists of two perpendicular sets of eight Pt wires (top and bottom). A bit of molecular memory (around 1000 molecules of an organic compound) is sandwiched at the crossing points between the higher and lower wire (Figure 2). The whole storage and switching units have an area of around 1 μm^2 with a wire-to-wire distance of about 40 nm. Although, the working principles of such a device are still under discussion, it is possible to "write" and to "read" the information at different voltages.[7b] Crossbar arrays based on nanowires may lead to addressable nanosystems.[7c]

Further interest in gridlike molecular architectures might arise from an alternative encoding concept called "cellular

[*] Dr. M. Ruben,[+] Dr. J. Rojo,[++] Dr. F. J. Romero-Salguero,[+++]
Dr. L. H. Uppadine, Prof. Dr. J.-M. Lehn
ISIS,Université Louis Pasteur
8, Allée Gaspard Monge, BP 70028
67083 Strasbourg cedex (France)
Fax: (+33) 390-245-140
E-mail: lehn@isis.u-strasbg.fr

[+] Institut für Nanotechnologie
Forschungszentrum Karlsruhe GmbH, PF 3640
76021 Karlsruhe (Germany)

[++] Dpto. Química Bioorgánica, IIQ, CSIC
Américo Vespucio s/n
41092 Sevilla (Spain)

[+++] Dpto. Química Orgánica, Universidad de Córdoba
Campus de Rabanales, edificio "Marie-Curie"
14014 Córdoba (Spain)

DOI: 10.1002/anie.200300636

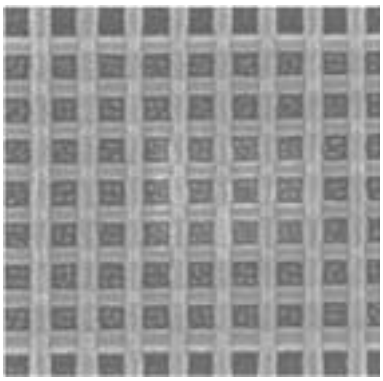

Figure 2. A 64-bit molecular storage device. The crossed-wire structure of the memory shows the eight top and the eight bottom Pt wires (wire-to-wire distance ca. 40 nm).[7a]

automata", in which molecules do not act as current switches but as structured charge containers.[8] Envisaged first for quantum dots, binary information is encoded in the charge configuration of a cell composed of a small number of differently charged redox centers, which are electronically communicating within the entity but are not completely delocalized (Robin-Day type II) (Figure 3). Each cell has two degenerate ground states, which can be interconverted by an internal electron density redistribution (e.g. by the transfer of two or more electrons within the cell). The electrostatic interaction of two neighboring cells (arranged in one, two, or three dimensions) lifts the given degeneracy and results in "1" or "0" states. Remarkably, the intercellular information exchange is purely based on Coulomb interactions and involves no current flow. If such interaction can be realized, this approach may enable a general purpose computation.[9]

From the standpoint of nanochemistry, the cells can comprise molecular or supramolecular entities. Multinuclear metal ion coordination arrays present particularly attractive features in this respect. The main interest arises from a self-organization strategy involving appropriate ligands and metal ions, which allows close control of the structural and physical properties of the resulting assemblies. Recent progress in molecular self-assembly processes has opened the way to generate extended supramolecular structures by spontaneous, but controlled build-up from their components.[3,10] Such self-fabrication techniques are of intense interest, due to the possibility of bypassing or complementing tedious (top-down) nanofabrication and nanomanipulation procedures.[3]

Jean-Marie Lehn was born in Rosheim, France in 1939. In 1970 he became Professor of Chemistry at the Université Louis Pasteur in Strasbourg and since 1979 he is Professor at the Collège de France in Paris. He received the Nobel Prize in Chemistry in 1987 for his studies on the chemical basis of "molecular recognition". Over the years his work led to the definition of a new field of chemistry, which he called "supramolecular chemistry". He is the author of more than 700 scientific publications, and member of many academies, institutions, and industrial bodies.

Francisco José Romero-Salguero was born in Baena, Spain, in 1967. He graduated both in chemistry (1990) and food science and technology (1992) from the University of Córdoba where he obtained his PhD in 1995. He then spent two years with Prof. J.-M. Lehn in Strasbourg as a postdoctoral researcher working on inorganic nanoarchitectures, before returning in 1998 to Córdoba where he is now an assistant professor in Organic Chemistry. His research interests focus on supramolecular synthesis and micro- and mesostructured catalysts for organic reactions.

Javier Rojo received his PhD degree under the supervision of Prof. J. C. Carretero at the University Autónoma, Madrid in 1995. He was a postdoctoral fellow with Prof. J.-M. Lehn at the Université Louis Pasteur in Strasbourg (1995–1998) and with Prof. L. W. McLaughlin at Boston College (1998–1999). In January 2000, he joined the Carbohydrate Group at the Spanish Research Council (CSIC) in Seville where he is now a permanent research scientist. In 2001 he was awarded a "Ramón y Cajal" fellowship. His research interests include supramolecular chemistry and molecular recognition of carbohydrates.

Mario Ruben studied Chemistry in Germany and Spain. He obtained his PhD in 1998 at the University of Jena, Germany, under the supervision of Prof. D. Walther. A DAAD postdoctoral fellowship brought him to Prof. J.-M. Lehn's research group at the ISIS-ULP in Strasbourg, France, where he worked on supramolecular coordination compounds. Since 2001 he is a group leader at the Institute of Nanotechnology, Karlsruhe. His research interests involve functional molecule-based systems and their implementation into operational nanosystems. He is the coordinator of several European networks (FUN-SMARTs; BIOMACH) dealing with molecular nanodevices.

Lindsay Uppadine obtained an M.Chem. degree from the University of Oxford in 1997. She stayed at Oxford for her doctoral research in the group of Prof. P. D. Beer, where she worked in the field of anion and ion pair recognition. She is currently a CNRS Postdoctoral Fellow in Prof. J.-M. Lehn's research group at the Université Louis Pasteur, Strasbourg.

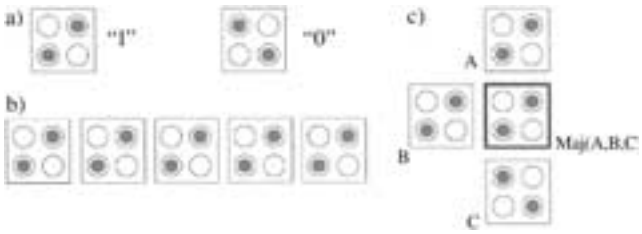

Figure 3. Schematic representation and working principle of "cellular automata". a) Coulomb repulsion keeps the electron density (dark) at antipodal sites resulting in the degenerate "1" and "0" state. b) A wire of "cellular automata" can be formed by a one-dimensional arrangement of cells. The intercellular Coulomb interactions force all units into the same state. c) Working principle of a majority logic gate consisting of three inputs (A, B, C) which converge to an output (Maj(A;B;C;)).[8]

2. General Concepts

Metallosupramolecular chemistry is an actively pursued area of research in supramolecular chemistry, which uses the interaction between organic ligands and metal ions to construct multicomponent and multinuclear coordination entities in the nanometer regime. It thus allows one to combine the properties of metal ions with those of the organic ligands in a defined structure with the potential for the generation of new properties not found in the individual components. A rich variety of metallosupramolecular architectures has been synthesized in the last few years, including helicates, rotaxanes, catenanes, and cages.[10]

The design of gridlike metal ion arrays rests on the directing coordination instructions, which are based on the coordination geometry of the metal ion and the structure of the ligand's coordination sites. It requires perpendicular arrangements of the ligand planes at each metal center. Given such a coordination environment around the metal centers, the linear and rigid extension of the ligand system from mono- to multitopicity will automatically lead to a gridlike two-dimensional coordination network with regularly arrayed metal ions. According to this general "leitmotif", metal ion arrays can be prepared in principle by careful prearrangement of the subunits using any set of metal ions and organic ligands possessing compatible coordination features. This requires ligands containing either bidentate or tridentate binding subunits in combination with metal ions possessing tetrahedral or octahedral (and in some cases bipyramidal) coordination geometry, respectively (Figure 4).

Two-dimensional gridlike coordination complexes lead to a well-defined 2D arrangement of an exact number of metal ions. A number of square $[n \times n]$ and rectangular $[n \times m]$ grids with $n,m \leq 4$ has been obtained for metal ions with tetrahedral as well as octahedral (and sometimes square-bipyramidal) coordination geometry (vide infra). Thus, a ligand with n coordination subunits is capable of forming a homoleptic $[n \times n]$ metalloarray, composed of $2n$ organic ligands and n^2 metal ions with an overall $[M_{(n^2)}L_{(2n)}]$ stoichiometry.[11] Mixtures of different ligands containing unequal numbers of coordination subunits n and m may, in addition to square arrays, yield

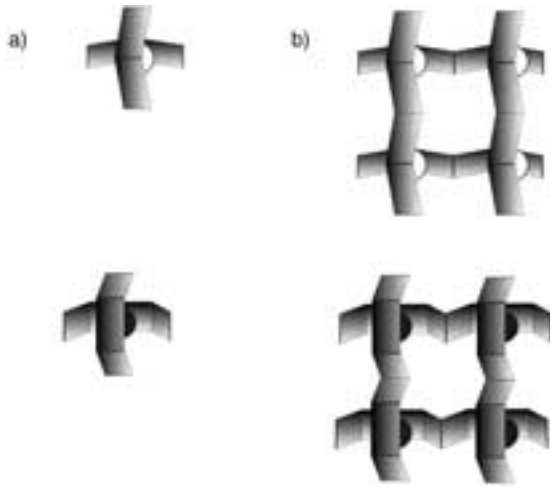

Figure 4. General principles and building blocks for perpendicular arrangement of the ligand L about a metal center M. a) $[M(L)_2]$ units are formed with monotopic ligands ($n=1$); b) gridlike metal ion arrays $[M_4(L)_4]$ are formed with multitopic ligands (here $n=2$). Coordination geometry of the metal ions: ○ tetrahedral, ● octahedral.

rectangular structures $[M_{(n\times m)}L_{(n+m)}]$ with a total of $(n + m)$ organic ligands and $(n \times m)$ metal ions. In incomplete gridlike coordination compounds, the available coordination sites are not fully occupied thus generating several *(p)* subsets of $[n \times n]$ or $[n \times m]$ arrays within the same coordination compound (Figure 5).

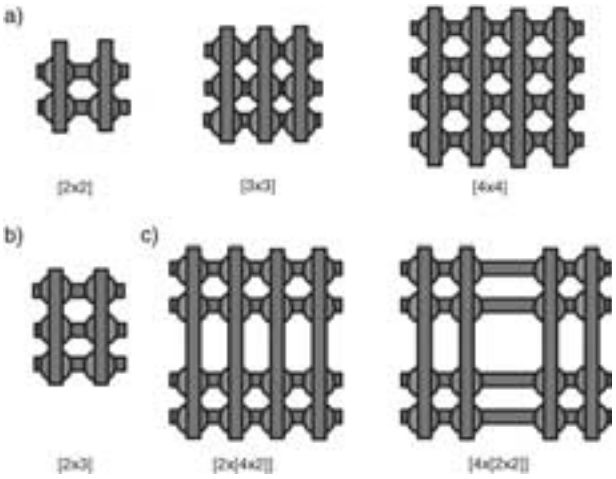

Figure 5. Different types of grid-type metal ion arrays: a) squares $[n \times n]$, b) rectangles $[n \times m]$, and c) incomplete architectures $[p \times [n \times m]]$.

In designing such metal ion arrays, the choice of organic ligands follows the coordination chemistry of the metal ions to be incorporated. In most cases, the coordination number of the metal ion is 4 or 6, with tetrahedral or octahedral coordination geometries. Appropriate design of the systems requires the choice of a ligand that presents an adequate number of binding sites in the coordination subunit to satisfy the coordination sphere of the metal ion. Most of the ligands used for the construction of grids, so far, are listed in Figure 6.

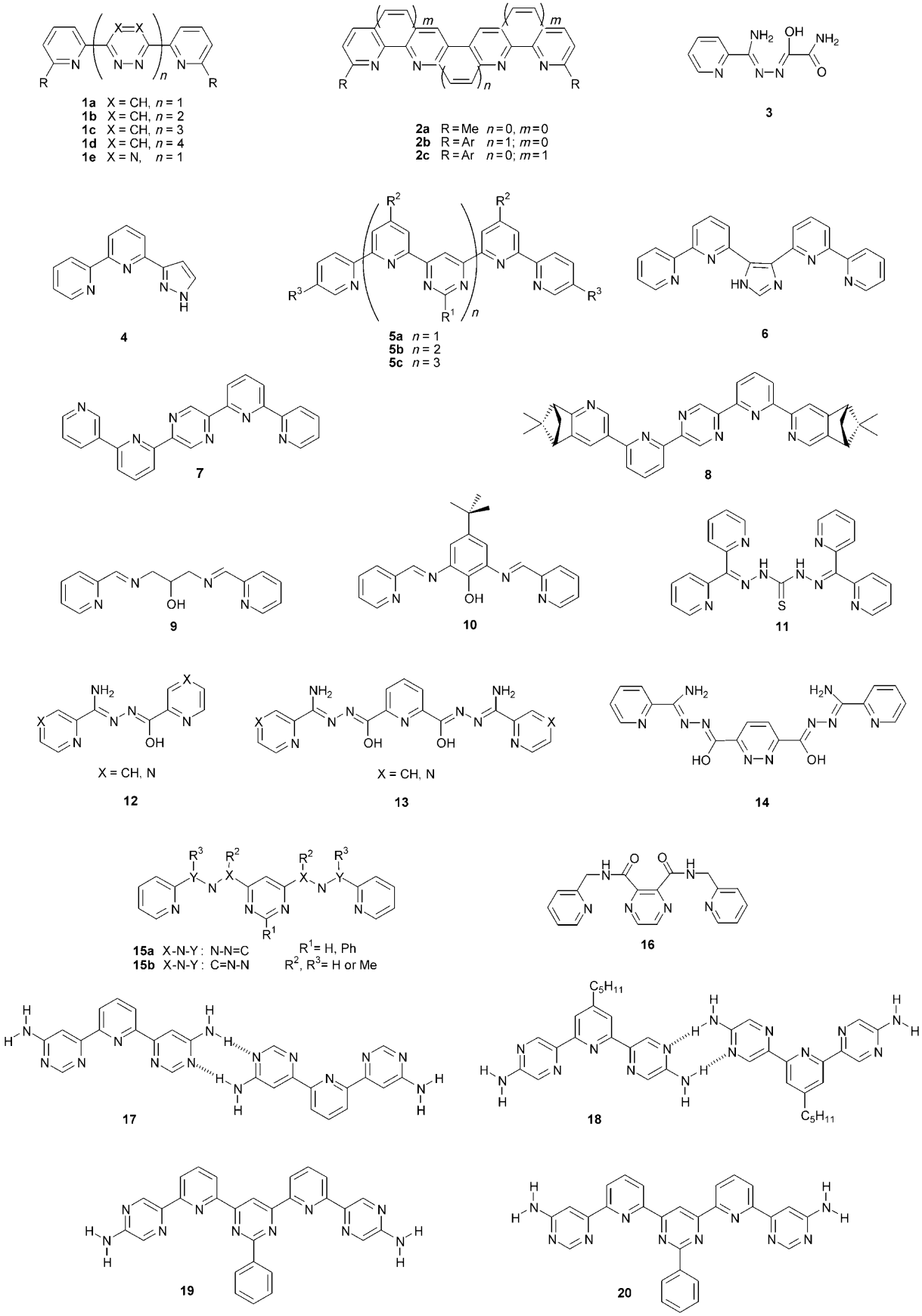

Figure 6. Ligands **1**–**20** employed in the self-assembly of gridlike metal ion arrays.

Those based on nitrogen donor ligands (such as bipyridine or terpyridine) are the most common, but ligands with sulfur- and oxo-bridging subunits have also been used.

Although some early examples can be identified,[12] grid-type architectures have only recently experienced active and coherent development and are mainly based on tetrahedrally and octahedrally coordinated metal complexes of azaaromatic ligands containing bidentate or tridentate subunits.[4–6, 13–26a]

In general, the matching information encoded in both the metal ions (nature, number, and disposition of electronic orbitals, charge, etc.) and in the organic ligands (number and nature of the donor atoms and the geometrical disposition, molecular conformations, rigidity, etc.) is interpreted during the self-assembly process and steers it to a mutually acceptable 2D architecture. All ligands shown in Figure 6 are chelating ligands, as their increased preorganization and stronger binding may result in cooperative effects during the self-assembly process. Furthermore, all these ligands contain rigid aromatic ring systems (mostly pyridine groups), which yield kinetically labile intermediates as well as thermodynamically stable end products with many M^{I}, M^{II}, and some M^{III} ions. The rigidity of these aromatic ring systems and their ability to participate in π–π interactions are further stabilizing factors for the gridlike array formation.

Energetically, the formation of the grid-motif competes with the generation of other types of structures (e.g. finite and infinite coordination oligo- and polymers). The defined gridlike array is favored enthalpically, since it maximizes the coordination site occupancy, as well as entropically, giving rise to the largest number of discrete entities. Furthermore, intercomponent interactions (π–π stacking, H-bonding) may contribute to achieving the correct alignment of all bricks.

Thus, the generation of grid-type arrays depends on three factors, which influence the self-assembly of metallosupramolecular architectures in general: 1) a robust set of coordination instructions that impose the correct (perpendicular) geometry and drive the process on the basis of the principle of maximal, optimally full, binding site occupancy;[27] 2) internal orienting effects, such as steric factors that hinder the formation of undesired entities, or stabilizing interactions (e.g. stacking) that channel the assembly to the desired product; 3) external factors such as binding of solvent molecule(s), counterion(s), or other species present in the environment. In addition to the energetic parameters, entropy favors the formation of the largest number of products.

These different factors promote the formation of the discrete, "closed" grid architectures over polymetallic entities, which might in principle also form. In addition to entropy considerations, such polymers are disfavored energetically by the remaining free sites at the ends ("sticky ends") of the polymer chains, as well as by the marked steric crowding that would occur between ligands bound to vicinal sites.

In addition to the assembly parameters mentioned so far, ligand substitutions provide the opportunity to fine-tune inherent functional properties (e.g. electronic, optical, magnetic, etc.). It is also possible to introduce a second coordination site on the ligand backbone, to enable multistep hierarchical organization of the self-assembly process.

It is crucial to note that the binding of metal ions to polyazaheterocyclic ligands involves major structural and energetical changes. Indeed, α,α′-connected aromatic azaheterocycles present a *transoid* orientation of the nitrogen sites around the C(α)–C(α′) bond, which is more favorable than the *cisoid* orientation required for metal ion coordination by about 25–30 kJ mol^{-1}.[26b] This feature has been implemented for designing heterocyclic "folding codons", in particular "helicity codons" that determine the shape of molecular strands.[26c] Thus, the free uncoordinated ligands based on α,α′-linked bipyridine or terpyridine moieties adopt a *transoid* conformation of the nitrogen atoms relative to the interheterocyclic C–C bond. The conversion of the all-*transoid* conformer into the energetically disfavored all-*cisoid* one upon metal complexation occurs at the cost of large amounts of conformational energy, which must be overcompensated by the interaction energy resulting from metal ion binding (Figure 7). For example, the change from an all-*transoid* to an all-*cisoid* form of the bis(terpyridine) ligand **5a** costs about 100 kJ mol^{-1} per ligand (i.e. 400 kJ mol^{-1} in total on formation of the corresponding $[2\times2]$ M_4 grid complex), and energy costs in excess of 1500 kJ mol^{-1} are attained on the self-assembly of the $[4\times4]$ Pb^{II}_{16} grid (see Section 3.3)!

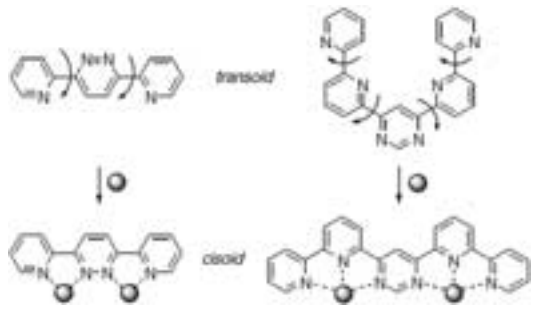

Figure 7. For the complete complexation, all binding sites of polyazaheterocyclic ligands must be present in the *cisoid* conformation. The required change in ligand conformation from all-*transoid* (uncoordinated ligand) to all-*cisoid* (coordinated ligand) is shown, for example, for the ligands **1a** (left) and **5a** (right).

In conclusion, the formation of gridlike architectures involves a subtle interplay of steric, enthalpic, and entropic effects, concerning both the ligand and the metal binding features. Thus, different metal ions and ligands can lead to the formation of different supramolecular coordination entities and self-assembly may result in several stable products partitioned under thermodynamic equilibrium. Only carefully designed systems of appropriate ligands and metal ions will lead to the self-assembly of gridlike metal ion arrays in a "programmed" fashion.

3. Grid-Type Metal Ion Arrays

3.1. [2×2] Metal Ion Arrays

The first report on the formation of $[2\times2]$ metal ion arrays based on tetrahedral coordination geometry involved

four *ditopic* ligands **1a** of the bis(pyridyl)pyridazine type arranged around four metal ions.[13a] Both Cu_4^I and Ag_4^I ion arrays (Figure 8) assemble spontaneously when the metal and ligand components are mixed in a 1:1 stoichiometry.[13]

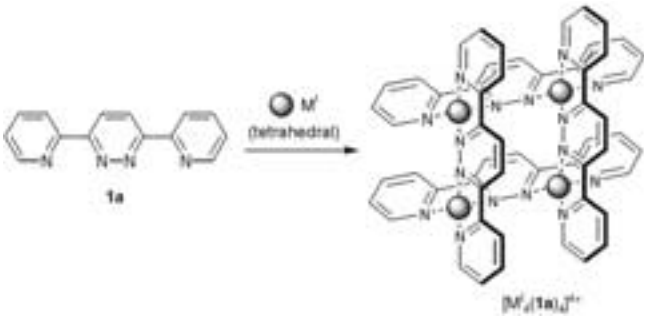

Figure 8. Schematic representation of the self-assembly process of ligand **1a** and tetrahedrally coordinating metal ions ($M = Ag^I$, Cu^I) leading to a [2×2] grid-type metalloarray $[M_4^I(\mathbf{1a})_4]^{4+}$.

The X-ray structure analysis of the $[Cu_4^I(\mathbf{1a})_4]^{4+}$ complex reveals a distorted rhombus with an almost planar arrangement of the metal ions in a distorted tetrahedral environment. The average Cu^I–N and Ag^I–N distances are about 2.0 and 2.3 Å, respectively, while the Cu^I–Cu^I distance is 3.57 Å and the Cu^I-Cu^I-Cu^I angles are approximately 79° and 101°.

An unusual self-assembled [2×2] metal ion array deviating from the general M_4L_4 stoichiometry was obtained by using the bis(phenanthroline)-based ligand **2c** and Cu^I ions. In addition to the expected $[Cu_4^I(\mathbf{2c})_4]^{4+}$ scaffold, two additional, uncoordinated "guest" ligands **2c** were sandwiched in the upper and in the lower groove of the complex by multiple C-H-N and π–π interactions.[14]

A [2×2] $Cu_4^{II}L_4$ metal ion array was obtained with the flexible ligand **3**; the two different ligand moieties are twisted by almost exactly 90° thus arranging the metal ions in a square-like fashion.[15]

Ligand systems containing terpyridine-like coordination sites enable the arrangement of octahedrally coordinating metal ions: a number of late first- and second-row transition metal ions (e.g. Mn^{II}, Co^{II}, Fe^{II}, Ni^{II}, Cu^{II}, Zn^{II}, Cd^{II}) as well as some main group metal ions (e.g. Pb^{II}) have been introduced into gridlike arrays.[4,6,16–17,24] The range of transition metals that can coordinate to ligand systems such as **5a** gives access to a wide variety of optical, electrochemical, photophysical, and magnetic properties. Furthermore, by using ligand system **5a**, these properties can be tuned by the choice of the different substituents R^1, R^2, and R^3 (Figure 9).

Ligand **5a** yields gridlike arrays of the metal ions with inter-metal distances of 6.0–6.5 Å between neighboring ions. The exchange of the central μ-pyrimidine group for an imidazole (**4**) or a pyrazole bridge (**6**) leads to only slightly shortened ion–ion distances.[18,19] However, the use of oxo- and sulfur-bridged ligands **9**–**12** (after deprotonation) resulted in more closely spaced metal ions with intermetallic distances of between 4.0 and 4.6 Å[20–22] (e.g. 4.04 Å in the phenoxo-bridged metalloarray $[Cu_4^{II}(\mathbf{10})_4]^{4+}$).

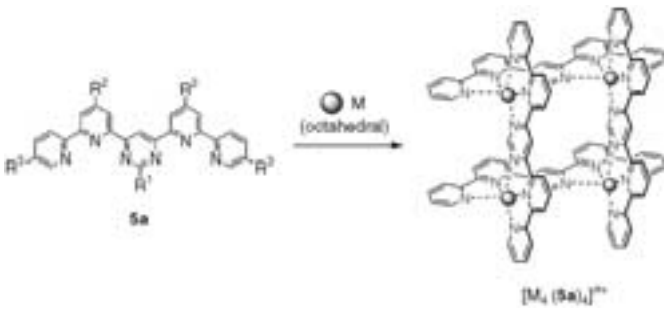

Figure 9. Schematic representation of the self-assembly of a [2×2] metal ion array from bis(terpyridine) ligands **5a** and octahedrally coordinating metal ions.

Ligand systems **15**[23] and **16** bearing acidic protons open the way to ionizable [2×2] arrays, whose self-assembly and properties can be influenced by the protonation state of the ligand (see Section 5.1.1 and 5.1.4).[24,25]

X-ray structure analyses show that anions can be located within the central cage of the [2×2] architecture, although this is not a prerequisite for the stability of the gridlike structure. On the other hand, a direct coordinative involvement of the anions was found in the [2×2] array $[Pb_4^{II}(\mathbf{5a})_4]^{8+}$, where a triflate anion is directly coordinated to each Pb^{II} center to fulfill the coordinative requirements of the large Pb^{II} ion.[17]

The controlled introduction of different metal ions at specific locations in a grid array is of great interest, because of the cross-over properties which may result from the presence of different metal ions in the same entity. Mixed ion [2×2] grid structures were obtained by a sequential synthesis protocol involving stereochemical features, for example, homochiral assembly of the intermediate *R* or *S* "corner" type intermediates (Figure 10). This self-assembly reaction is reminiscent of the "Coupe de Roi", in which an achiral object is divided into two identical homochiral components.[26a]

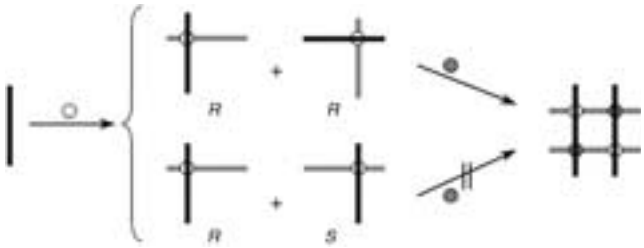

Figure 10. Self-assembly of a chiral heterobimetallic [2×2] grid from two cornerlike homochiral precursors (*R* + *R*) or (*S* + *S*).[26a] The resulting grid is achiral in the homometallic case ("Coupe de Roi" process) and chiral in the heterobimetallic case.

A [2×2] grid-type structure with two pairs of unlike metal ions may exist as either the *anti* or *syn* topoisomer. It is not possible to select a priori which form is generated by simply mixing together the components; however, the *anti* topoisomer, with diagonally located identical ions, can be obtained selectively from a precursor complex consisting of

two terpyridine-type ligands (e.g. **5a**) and a strongly coordinating metal ion such as Ru^{II} or Os^{II} (to give for example $[M^{II}(\mathbf{5a})_2]$). They contain two vacant sites, which combine with a second metal ion M'^{II} of lower coordinative binding strength to yield a heterometallic $[2\times2]$ complex as the thermodynamic product. The combination of homochiral fragments leads to a C_2-symmetric array (e.g. $[M^{II}_2M'^{II}_2(\mathbf{5a})_4]$) in a process displaying spontaneous chiral discrimination.

Such a methodology represents sequential self-assembly and introduces different metal ions in order of increasing coordinative lability. Thus, a system containing three different metal ions was isolated from an equimolar mixture of Ru^{II} and Os^{II} "cornerlike" fragments $[Ru^{II}(\mathbf{5a})_2]$ and $[Os^{II}(\mathbf{5a})_2]$ in the presence of Fe^{II} ions.[26a]

An even more sophisticated, three-tiered synthesis, incorporating regioselective, redox, and chiroselective features, was used to construct $[Co^{III}_2M^{II}_2(\mathbf{15a})_4]$ grid-type arrays (M^{II} = Co^{II}, Zn^{II}, Fe^{II}) based on the bis(hydrazone) ligand-type **15a** (R^2 = H and Me, $R^2_{left} \neq R^2_{right}$) containing both ionizable and nonionizable compartments.[24b] As a consequence, the oxidation state of cobalt could be modified according to the charge on the hydrazone moiety.

The first stereoselective synthesis of a $[2\times2]$ metal ion array was achieved by using the chiral ligand system **8**. The "chiralization" of the parent ligand **7** was carried out by the introduction of pinene moieties, which gives access to both ligand diastereomers of **8** (only one is shown in Figure 6). The reaction of **8** with Zn^{II} ions delivers the tetranuclear (all-Δ)$[Zn_4((R,R)\text{-}\mathbf{8})_4]^{8+}$ metal ion array as the major product in good diastereomeric excess.[28]

3.2. [3×3] Metal Ion Arrays

The first $[3\times3]$ M_9 grid, $[Ag^{I}_9(\mathbf{1b})_6](OTf)_9$, was obtained in high yield by self-assembly of six equivalents of the tritopic ligand **1b** with nine equivalents of silver(I) ions.[29] Because of the deviation of the coordinated ligand planes from the ideal $\gamma = 90°$, the resulting $[3\times3]$ Ag^{I}_9 array forms a trapezoid with corners (angle Ag-Ag-Ag) of about 73° and 107°.

The self-assembly of ligand system **5b** with octahedrally coordinating metal ions gave mainly incomplete metal ion arrays (see Section 3.5).[30a] Some evidence for $[3\times3]$ gridlike species was only obtained by electroscpray mass spectrometry in solution for the very large metal ions such as Pb^{II} or Hg^{II}.[30b] The behavior of **5b** may be ascribed to ligand bending due to the pinching of the binding subunit on coordination of transition-metal ions.[30c] Conversely, large metal ions such as Pb^{II} or Hg^{II} cause less pinching so that the ligand is less distorted from a linear arrangement, resulting in a less strained grid architecture.

The aromatic polytopic ligands **13** readily self-assemble with Mn^{II}, Cu^{II}, and Zn^{II} salts to produce nonanuclear $[3\times3]$ gridlike metal ion structures, in which the ligands are arranged in parallel sets and alkoxide bridging groups are located between adjacent metal ions. Spectroscopic and other evidence indicate that similar metalloarrays are produced with Ni^{II}, Co^{II}, and Fe^{III} ions, but not with Pb^{II} ions.[5,21] The cationic structures consist of a homoleptic $[M_9(\mathbf{13})_6]^{n+}$ complex in a roughly planar square array with metal–metal distances of about 4.0–4.3 Å (Figure 11).

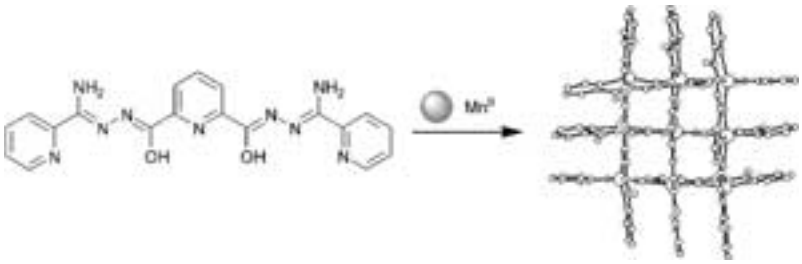

Figure 11. Self-assembly of the $[3\times3]$ metal ion array $[Mn^{II}_9(\mathbf{13})_6]^{6+}$, the molecular structure of which is depicted on the right.[5a]

3.3. [4×4] Metal Ion Arrays

The largest square grid reported to date, $[Pb^{II}_{16}(\mathbf{5c})_8](OTf)_{32}$, is formed quantitatively from eight equivalents of the tetratopic tridentate ligand **5c** and sixteen equivalents of Pb^{II} ions.[17] This remarkable species arises from the self-organization of 24 precursors and involves the formation of 96 coordination bonds. This example highlights the power of metallosupramolecular chemistry to create complex structures through self-assembly in a single operation.[6]

The final composition of the $[4\times4]$ Pb_{16} array consists of 8 molecules of ligand **5c**, 16 lead(II) ions, 16 triflate ions, and 8 coordinated water molecules; 16 further triflate ions and 1 molecule of water are located in close proximity. The eight ligands **5c** are arranged into two perpendicularly disposed sets of four outer and four inner ligands, resulting in a set of four $[2\times2]$ subgrids rather than a regular $[4\times4]$ grid (Figure 12).

The four inner ligands allow considerable overlap between the aromatic groups situated in a face-to-face stacking arrangement, with an average π–π stacking distance of 3.62 Å corresponding to the van der Waals contacts. The Pb^{II} ions form a saddle arrangement with an average Pb···Pb distance of 6.3 Å and average inner angles of 89.5°. The coordination polyhedron around the Pb^{II} ions reveals a hemidirected structure, and all of them present a distorted seven-, eight- or nine-coordinate geometry. The open faces of the metal ions are oriented towards the interior of the four $[2\times2]$ Pb^{II}_4 grid subsets and are occupied by one or two of the 16 internally coordinated triflate ions. Some of the internal triflate ions act as bridges between two adjacent Pb^{II} ions. Thus, each square of four Pb^{II} ions is linked on three sides by bridging triflate ions, whereby the remaining coordination sites at the Pb^{II} ions are filled with nonbridging triflate ions or water molecules.

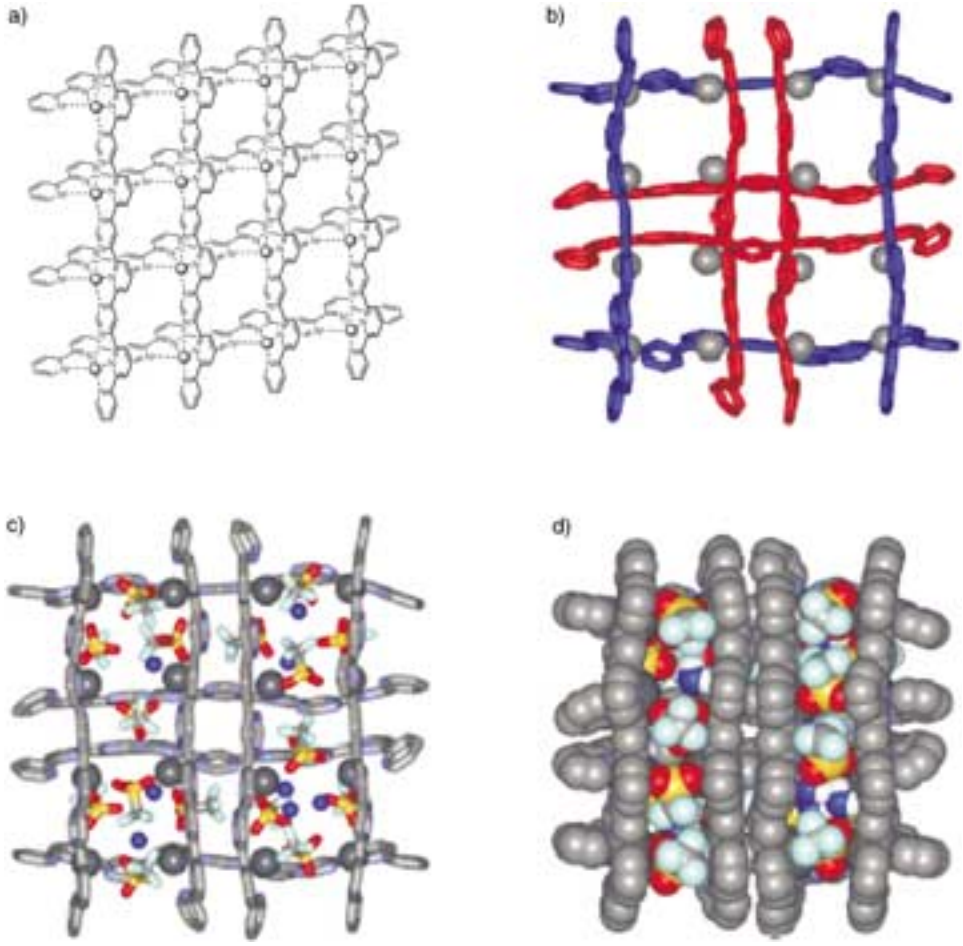

Figure 12. A [4×4] grid assembled from eight tetratopic ligands **5c** and sixteen Pb^{II} ions: structure (a) and ball-and-stick model (b) of the $[Pb^{II}_{16}(\mathbf{5c})_8]$ framework. The framework with coordinated triflate anions and water molecules as ball-and-stick model (c) and as space-filling model (d).[6]

3.4. Rectangular [n×m] Metal Ion Arrays with (n≠m)

The construction of a rectangular grid involves the self-assembly of two ligands with a different number of coordination sites. In this case, however, the reactions with different ligands could lead to mixed homo- and heteroleptic products, as described, for example, for the reaction of the di- and tritopic ligands **1a** and **1b**, respectively, and $AgCF_3SO_4$.[31a] When a 3:2:6 stoichiometric ratio of these components was used, a [2×3] grid was obtained as major compound (90%) in nitromethane solution, together with minor amounts of a [2×2] and a [3×3] grid (8% and 2%, respectively; Figure 13).

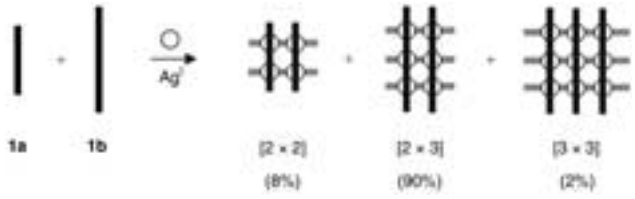

Figure 13. Synthesis of a [2×3] array from three ditopic ligands **1a**, two tritopic ligands **1b**, and six Ag^I metal ions.[31]

This preferential assembly could be due to the lower stability of the metal–ligand coordination bonds at the central coordination site of the [3×3] grid as well as from solvation and thermodynamic parameters. In the [2×3] grid structure, the silver ions are arranged on a [2×3] rhombohedrally distorted rectangular matrix with an average Ag–Ag distance of 3.75 Å.[31]

Rectangular [2×2] M^{II} arrays can be also obtained where ligands of type **12** (see Figure 6) coordinate in different conformations with different bridging groups.[21a,31b,32]

3.5. Incomplete Metal Ion Arrays [p×[n×m]]

The self-assembly of the pentatopic ligand **1d** with Ag^I ions, aimed at constructing a [5×5] grid, ultimately led to the formation of two isolable polynuclear architectures: an incomplete grid-type species (Figure 14) and a quadruple-helicate, which crystallize side-by-side from an equilibrating mixture of the complexes in solution.[33] Twisting around the central bond in the set of five parallel ligands releases a significant amount of strain so that a [2×[2×5]] species is generated rather than the complete [5×5] grid.

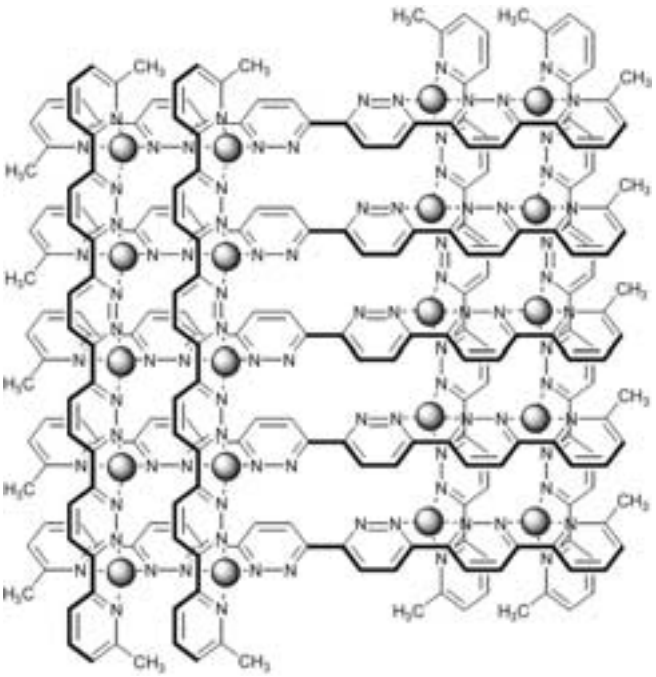

Figure 14. The [2×[2×5]] Ag^{I}_{20} grid assembled from nine pentatopic ligands **1d** and twenty Ag^{I} ions.[33]

The X-ray structure analysis of the icosanuclear complex $[Ag^{I}_{20}(\mathbf{1d})_9]^{20+}$ reveals two [2×5] Ag^{I}_{10} rectangular subgrids located on opposite sides of an array of parallel ligands twisted into a *transoid* conformation across the central pyridazine–pyridazine bond, one above and one below the mean plane through the 20 Ag^{I} ions. This arrangement may be described as a "grid-of-grids" [2×[2×5]] with a distorted rhombohedral geometry of 23.3×23.3 Å, where within each column the average Ag^{I}–Ag^{I} separation is 3.73 Å along each ligand and 3.93 Å between the inner Ag^{I} ion of each [2×5] column.[33]

Attempted construction of [3×3] grid-type architectures with bis(terpyridine)-type ligands **5c** revealed that in most cases only a [2×3] complex comprising five ligands and six metal ions could be obtained (Figure 15).[30a] In these [2×3] structures, all sites are occupied by metals except for a vacant central row. Although some evidence for the formation of [3×3] grid-type complexes could be obtained for large metal ions, such as Hg^{II} and Pb^{II}, the enhanced ligand distortion for metal ions with smaller ionic radii becomes a decisive factor in determining the thermodynamically most stable complex, which in this case is the intermediate [2×3] grid-type structure with only a few of the central binding sites occupied. Thus, the predominant self-assembly of [2×3] architectures is a deviation from the "maximum coordination site occupancy" principle and is caused by ligand strain. Often in these cases, various other complexes representing incompletely assembled grids and cyclic structures were detected in lesser amounts.

The X-ray structure analysis of the [2×3] Co^{II}_6 grid $[Co^{II}_6(\mathbf{5b})_5]^{12+}$ (R^1 = Ph) consists of five ligands arranged into two sets.[30a] The first set includes three parallel ligands at a distance of 6.7 Å which are twisted into a *transoid* conformation about the two central pyrimidine-pyridine-pyrimidine C–C bonds. The central binding site of each is unoccupied. The second ligand set is composed of two units markedly warped, whose nitrogen atoms are fully coordinated and in a *cisoid* conformation. The Co^{II} ions are arranged into two rows of three ions with a Co–Co separation of 6.5 Å. The distance between two Co^{II} atoms in different rows is 13.8 Å.

A dodecanuclear metal ion array was obtained in the self-assembly of ligand **14** with Cu^{II} ions.[34a] It is based on a [4×4] grid-motif, with an exclusive occupation of the peripheral coordination sites (leaving the inner four positions empty).

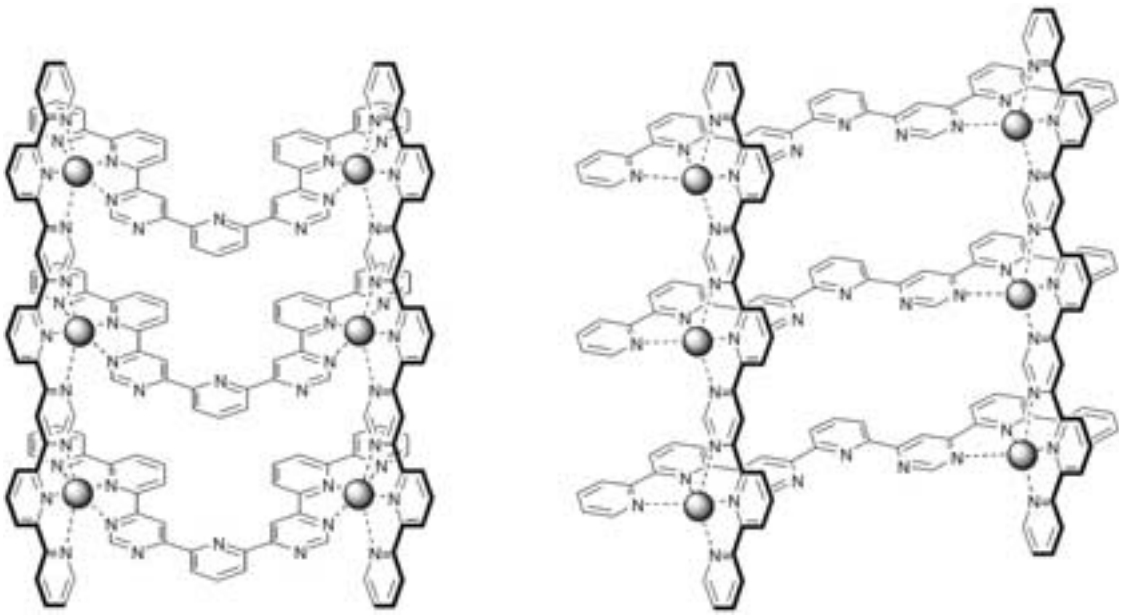

Figure 15. Two structures of the [2×3] incomplete grid architectures obtained by self-assembly of ligand **5b** and metal ions such as Co^{II}, Zn^{II} or Fe^{II}[30a]

More recently, the same basic type of ligand system was used to generate a $[4\times[2\times2]]$ Pb^{II}_{16} array.[34b]

4. Mechanistic Features of the Self-Assembly Process

The nature of the emerging species during the self-assembly of the different grid-type complexes has been studied in solution and in the solid-state. A self-assembled collection of species is obtained upon mixing of the bis(bipyridine)-based ligand **2a** and Cu^{I} ions. Detailed analysis of the resulting equilibrium mixture indicated the presence of three major species: a double-helical architecture, a triangular complex, and square $[2\times2]$ grid complexes (Figure 16). These represent the output of a dynamic combinatorial library of supramolecular components, from which the double-helical complex could be trapped by crystallization.[35] Very similar observations were made for ligand systems **7** with Zn^{II} ions, which yielded an equilibrium mixture of triangular and tetranuclear reaction products.[28]

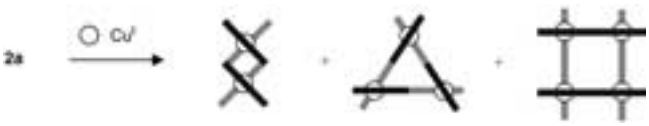

Figure 16. Self-assembly of an equilibrating mixture of the double-helical, triangular, and square $[2\times2]$ grid complexes from **2a** and Cu^{I} ions. Gray bars correspond to ligands located on the underside.[35]

The formation pathway of the $[3\times3]$ $[Ag^{I}_{9}(\mathbf{1b})_6]^{9+}$ metal ion array has been extensively studied by NMR spectroscopy.[36] This self-assembly process involves several intermediates, which are generated at different metal/ligand stoichiometries. A mixture of several unidentified species is observed at low $Ag^{I}/(\mathbf{1b})$ ratios until $Ag^{I}/(\mathbf{1b})\approx1{:}1$ is reached, when two complexes of $[Ag^{I}_{n}(\mathbf{1b})_n]^{n+}$ type are mainly present. They are characterized by an intertwined structure and a *transoid* arrangement of ligands. At $Ag^{I}/(\mathbf{1b})\approx6{:}5$ a species $[Ag^{I}_{6}(\mathbf{1b})_5]$ has been identified which has three ligands in *transoid* form and two ligands in the all-*cisoid* form. Further addition of Ag^{I} ions leads to the conversion of this intermediate into the final $[Ag^{I}_{9}(\mathbf{1b})_6]^{9+}$ grid presumably through a $[Ag^{I}_{6}(\mathbf{1b})_5]^{6+}$ entity with all five ligands in the all-*cisoid* form. These observations imply an overall positive cooperativity and a robust structure for the final $[3\times3]$ $[Ag^{I}_{9}(\mathbf{1b})_6]^{9+}$ complex (Figure 17).

The templating effect of certain anions upon the construction of metallosupramolecular nanostructures was clearly recognized for circular helicates and results from the operation of dynamic combinatorial diversity.[37] The self-assembly of Ni^{II} or Zn^{II} ions with ligand **1e** in the presence of

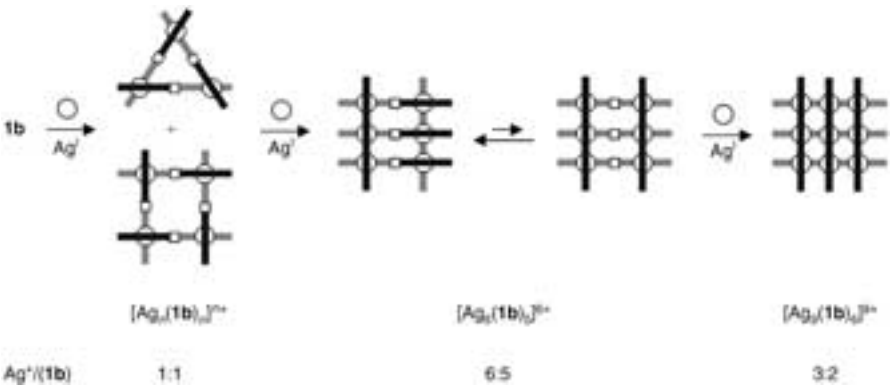

Figure 17. Self-assembly pathway for the $[3\times3]$ array $[Ag_9(\mathbf{1b})_6]^{9+}$. The uncomplexed bipyridine-type sites are noted by an open square; they are expected to adopt the more stable *transoid* arrangement.[36]

BF_4^- or ClO_4^- ions leads to the formation of the $[2\times2]$ grid complexes (Figure 18).[38] The metal ions have octahedral coordination geometry, with four of the coordination sites occupied by two ligands and the other two positions by acetonitrile and/or water molecules.

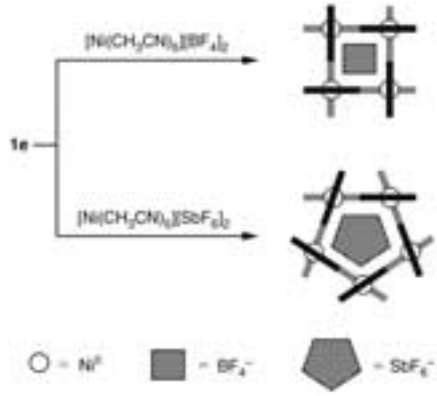

Figure 18. Templating effect of the anions BF_4^- and SbF_6^- on the formation of metallosupramolecular nanoarchitectures with the ligand **1e**.

An anion is encapsulated within the cavity of these grids. Moreover, the ligands are disposed in an interwoven manner, giving rise to a chiral grid which could be spontaneously resolved as chiral crystals.[38b] However, the self-assembly of the same ligand with Ni^{II} ions in the presence of a larger counterion such as SbF_6^- resulted in the formation of a molecular pentagon consisting of five ligands and five Ni^{II} ions (Figure 18).[39]

As it has been stressed earlier, correct self-assembly implements both maximal site occupation and pathway selection (or orientation) by the introduction of appropriate substitution. The nature of the solvent and the concentration of reagents may also affect the output of the self-assembly process. For example, ligand **2a** (R = H) in the presence of Cu^{II} ions in a 1:1 ratio in acetonitrile gives equilibrating mixtures of a $[2\times2]$ grid and a hexagonal architecture

(Figure 19).[40] At increased concentrations in acetonitrile, the relative amount of hexamer increases. Its crystal structure revealed the presence of acetonitrile molecules and hydroxo groups bound to the Cu^{II} centers, which are therefore five-coordinate. On the other hand, only the [2 × 2] metal ion array could be detected in nitromethane. Replacement of nitromethane by acetonitrile and vice versa indicated the reversible switching between a solution containing either the grid alone or an equilibrating mixture of the grid and the hexameric ring. This process displays three remarkable features: 1) self-assembly with substrate binding, 2) dynamic combinatorial structure generation, and 3) environment-sensitive behavior resulting in a process of adaptive self-assembly.[40]

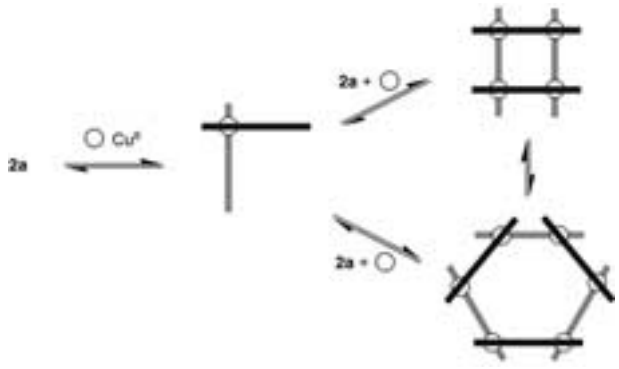

Figure 19. Adaptive self-assembly of the [2 × 2] grid $[Cu^{II}_4(\mathbf{2a})_4]^{8+}$ and the hexameric cyclic complex $[Cu^{II}_6(\mathbf{2a})_6]^{12+}$ from ditopic ligand **2a** (R = H) and Cu^{II} ions. The products exist in a solvent-dependent equilibrium.[40]

On the basis of the results obtained for many different grid self-assembly experiments, it can be stated that $[n \times n]$ grid-type complexes of high nuclearity may be disfavored by: 1) the imposition of a *cisoid* conformation for all ligands; 2) the bent, domelike shape in two perpendicular directions ("pinching-in") of the ligand; and 3) the presence of central metal ion coordination sites containing poorer donor atoms. On the other hand, they are favored by: 1) the trend towards establishing the highest number of coordination interactions and therefore towards maximum site occupancy; 2) maximization of stabilizing π–π contacts between ligands, and 3) the interaction with included anions or guest molecules. Thus, a subtle interplay between metal coordination, strain, and steric demand of the ligands as well as external factors, reaction conditions, and the nature of the counterions determines the product of the self-assembly.

5. Multistability and Addressability

High density information storage and informatics on the nanoscale may take advantage of a designed exploitation of intrinsic functional molecular properties and their modifications, such as size, multiplicity, and heteronuclearity as well as different redox, magnetic, or spin states. Planar multicenter transition-metal complexes appear to be very attractive candidates for the design of multilevel information storage devices, because they could fulfill intrinsically two important prerequisites for nanoscale memory devices: 1) multistability and 2) addressability.

5.1. Multistability

5.1.1. Redox States

The first report on the electrochemical properties of a [2 × 2] gridlike complex concerned the copper(I) complex $[Cu_4(\mathbf{1a})_4](BF_4)_4$, which exhibits seven reversible single-electron reduction waves.[13a] The electrochemical behavior of a family of tetranuclear gridlike oligopyridine complexes of the general formula $[M^{II}_4(\mathbf{5a})_4]^{8+}$ displays well-resolved multiple one-electron reductions in all complexes investigated.[41] Furthermore, the introduction of electron-donating or -attracting groups into the ligands tunes systematically the potential of the first reduction. As a consequence, one Co^{II}_4 member of this family exhibits up to twelve well-resolved reversible one-electron processes at room temperature, which appears to be the most extended redox series known for well-characterized molecular compounds.[41]

The rather low values of the redox potentials are of importance for the stability of the multielectron species generated and thus for their possible applications as devices presenting multiple electronic levels. Spectroelectrochemical experiments revealed that the reductions take place on the coordinated ligands in all cases; no reduction of the metal centers was observed in the accessible potential range. Interestingly, the Co^{II}_4 species exhibited an amazing regularity in the disposition of the reduction waves, as well as a remarkable stability and reversibility towards reduction (Figure 20). In contrast, analogous Mn^{II}_4 arrays with M^{II} = Fe^{II}, Ru^{II}, Os^{II}, Zn^{II}, and Mn^{II} were found to be more sensitive towards decomposition and to produce more complex reduction schemes. The nature of the M^{II} ions in gridlike complexes plays a very important role for mediating electronic communication within the metalloorganic supramolecular array.[41]

The oxidation of the manganese(II) [3 × 3] array $[Mn_9(\mathbf{13})_6]^{6+}$ was studied by cyclic voltammetry and coulometry.[21b] A series of $Mn^{II} \rightarrow Mn^{III}$ oxidation waves was found,

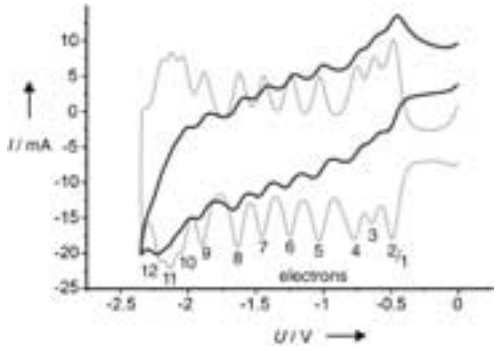

Figure 20. Plot of the sequential 12-electron reduction of the $[Co^{II}_4(\mathbf{5a})_4]^{8+}$ array in dimethylformamide (DMF) at room temperature. Black line: cyclic voltammogram (CV); gray line: deconvolution of the CV; reference: Fc^+/Fc. [41b]

and the number of electrons per wave gave an insight into the sequence of oxidations in the array (Figure 21). A four-electron oxidation event occurs at +0.61 V, tentatively assigned to simultaneous oxidation at the grid's four equivalent corners. Four additional oxidation waves at +0.92, +1.13, +1.33, and +1.53 V were attributed to the remaining edge-located Mn atoms, but oxidation of the central ion was not observed. Spectroscopic changes were correlated to an increasing proportion of positive charge on the array.

The protonation state of the ligand can also be used to manipulate the electrochemical properties of the gridlike array. For example, protonic modulation of redox properties has been achieved for ionizable [2×2] Co_4^{II} and [2×2] Co_4^{III} grids based on ligand **15a** ($R^2 = H$).[42]

Thus, the [2×2] Co_4^{II} and [3×3] Mn_9^{II} arrays are intriguing electron reservoirs, representing multiredox state electronic systems. Future studies may uncover a system presenting the features required for investigation into nanometric devices used for data representation, and addressable either locally, at a given metal or ligand site, or through the overall redox state (see Figure 21 and ref. [3a]).

5.1.2. Magnetic States

A new type of molecular material has recently emerged based on polynuclear metal complexes called "single-molecule magnets" (SMMs). SMMs possess slowly relaxing magnetic moments, a prerequisite for use in future magnetic information storage devices. This class of molecules exhibits a unique concomitance of both macroscopic (e.g. magnetism) and quantum regime properties (e.g. quantum tunneling) within monodispersed molecular entities.[43]

The principal interest for potential use of SMMs as magnetic memory units arises from their size, undercutting the paramagnetic limit of conventional information storage materials, and from the presence of an energy barrier for the reversal of the direction of the molecular magnetization. The origin of magnetism in the SMMs is the spin(s) on individual metal ions, which couple to give rise to a high-spin ground state. The SMMs have an axial zero-field splitting, which leads to a double well potential with an energy barrier between "spin-up" and "spin-down" states. The final height U of the barrier is determined by $U = |D| S^2$, where D is the zero-field splitting parameter and S the resulting spin quantum number. Consequently, SMMs display hysteresis in their magnetic susceptibility versus external magnetic field loop (so far, only at very low temperature), which might be used in molecular data storage.[44]

In conclusion, to achieve such molecular magnetic data storage, the respective molecule has to possess 1) a high total spin quantum number S and 2) a high Ising-type anisotropy barrier arising from a negative zero-field splitting parameter D. A high spin quantum number S demands intramolecular ferromagnetic coupling of the involved metal ion spins. The commonly found antiferromagnetic coupling "destroys" the spin densities and renders completely antiferromagnetic-coupled molecules useless for magnetic information storage. Usable SMMs exhibiting AF coupling are molecular ferrimagnets, where the overall spin ground state is a result of the noncompensation of spins. A negative zero field splitting parameter D depends on the electronic nature of the metal ions involved (e.g. Mn^{III}) in combination with the low overall symmetry of the molecule.

The first and still most prominent example exhibiting SMM-like behavior was a spin cluster referred to in the literature as "Mn_{12}".[45] Later, other molecular compounds such as "Fe_8", "Fe_{19}", or "Mn_4" joined the SMM family.[46]

The ongoing search for SMMs exhibiting high anisotropy barriers (preferentially above room temperature to overcome the thermal fluctuation) is driving the increasing interest in the magnetic properties of spin bearing metal ion arrays. Thus, the [2×2] Co_4^{II} entity was shown to represent an isolated magnetic domain, a model system for studying magnetic interactions in discrete entities.[47] However, the whole series of [2×2] M_4^{II} ion arrays $[M_4^{II}(\mathbf{5a})_4]^{8+}$ (M = Mn^{II}, Co^{II}, Ni^{II}, and Cu^{II}) exhibited exclusively weak antiferromagnetic intramolecular exchange couplings. Evidently, the μ-pyrimidine unit in ligand **5a** is able to mediate antiferromagnetic but not the necessary ferromagnetic magnetic exchange couplings. The weak magnitude of the coupling parameter J can be attributed to the rather long metal–metal distances of around 6.5 Å.[48] The change to the negatively charged μ-phenoxo bridging group in the [2×2] $[Cu_4^{II}(\mathbf{10}^-)_4]^{4+}$ compound leads to even weaker antiferromagnetic couplings.[20]

Ferromagnetic exchange coupling was found in the μ-alkoxo-bridged $[Cu_4^{II}(\mathbf{12})_4]^{4+}$ grid complex, but only antiferromagnetic couplings were observed for all further spin-bearing ions assembled with the same ligand.[21] Related to this work, the tritopic ligand **13** (X = CH) gave access to a ferromagnetically coupled Cu_8^{II} pin-wheel [2×2] gridlike complex (Figure 22).[49]

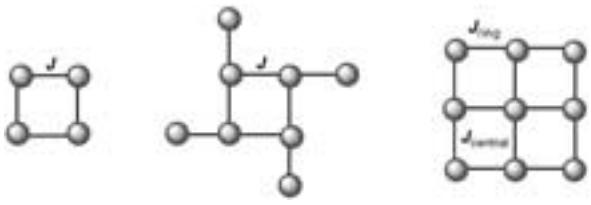

Figure 22. Definition of the coupling constants J in [2×2] arrays (left), [2×2] "pin-wheel" arrays (middle), and [3×3] arrays (right).

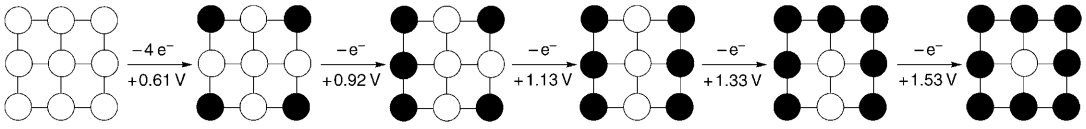

Figure 21. Proposed oxidation sequence of manganese ions in the [3×3] metal ion array $[Mn_9(\mathbf{13})_6]^{6+}$ (○ Mn^{II}, ● Mn^{III}), based on experimental data.[21b]

The magnetic properties were thoroughly investigated for a series of nonanuclear [3×3] grid complexes incorporating doubly μ-O bridging ligands **13**.[21c] Some of the $[M_9^{II}(\mathbf{13})_6]^{n+}$ systems exhibit magnetic features which can be interpreted as a combination between ferromagnetic and antiferromagnetic exchange processes. The relative contributions of ferromagnetic and antiferromagnetic coupling vary according to the temperature (e.g. the ferromagnetic behavior is more pronounced at low temperatures because all antiferromagnetic contributions are effectively coupled to a small spin ($S=0$) ground state). To explain the combined antiferromagnetic/ferromagnetic coupling situation found in these metal ion arrays, the [3×3] grid can be considered as the sum of a ring of eight metal ions coupled to the central metal ion yielding two different exchange constants J_{ring} and $J_{central}$ (Figure 22). The $[Mn_9^{III}(\mathbf{13})_6]^{15+}$ system involves $|J_{ring}| \gg |J_{central}|$, and displays only antiferromagnetic behavior.[5b] However, the orbital based magnetic orthogonality leads to the simultaneous observation of both exchange modes in the Cu_9^{II} case, with dominant ferromagnetic exchange coupling at low temperatures.[5,50a]

There is currently no evidence for an anisotropic energy barrier in either the ferromagnetically coupled Cu_4^{II} grid arrays or the antiferromagnetically/ferromagnetically coupled Cu_9^{II} systems. However, a recent hint for magnetic anisotropy was given by the observation of metamagnetic-like behavior in antiferromagnetically coupled [3×3] Mn_9^{II} and [2×2] Co_4^{II} arrays.[50b,c]

The investigation, understanding, and manipulation of magnetic coupling between metal ions in metallogrid complexes is a first step towards the potential use of gridlike arrays in information storage devices. The discovery of ferromagnetic coupling in some Cu^{II} arrays is encouraging, although ways to introduce a magnetic anisotropy barrier have still to be explored. The choice of donor atoms, bridging groups, paramagnetic metal ions, and systematic synthetic design strategies (in contrast to the mostly serendipitous syntheses of magnetic oxo clusters) might render such supramolecular metallogrid arrays well suited for magnetic data storage at the nanometric scale.

5.1.3. Electronic Spin States

Among the physical properties that may be considered for magnetic molecular data storage systems, the spin transition (ST) phenomenon between the low-spin (LS) and the high-spin (HS) state of Fe^{II} ions is an attractive process to enable molecular memory effects.[51] Spin transition systems possess an unique concomitance of possible "write" (temperature, pressure, light) and "read" (magnetic, optical) parameters.[52] Investigations along these lines revealed ST behavior in several Fe_4^{II} gridlike [2×2] arrays (e.g. $[Fe_4^{II}(\mathbf{5a})]^{8+}$). The internal spin states of the incorporated Fe^{II} ions could be switched between the diamagnetic (LS; $S=0$) and the paramagnetic (HS; $S=2$) state by applying external field triggers (temperature, pressure, light) on macroscopic samples.[53]

The occurrence of ST in [2×2] gridlike ion arrays of the type $[Fe_4^{II}(\mathbf{5a})_4]^{8+}$ depends directly on the nature of the substituent R^1 in the 2-position of ligand **5a**. All metal ion arrays with substituents R^1 favoring relatively strong ligand fields (R^1 = H; OH) remain entirely in the diamagnetic LS state throughout all studied temperatures. Only complexes bearing substituents R^1 that attenuate the ligand field by steric (and to a lesser extent electronic) effects (R^1 = Me, Ph) exhibit temperature triggered spin transition (Figure 23). The

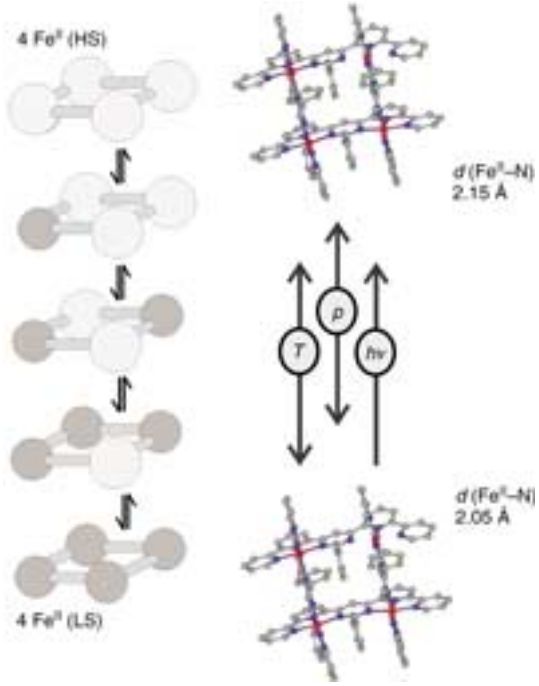

Figure 23. General switching scheme between the Fe^{II} spin states in the $[Fe_4^{II}(\mathbf{5a})_4]^{8+}$ metal ion arrays triggered by temperature, pressure, and light. The averaged Fe–N bond lengths in the 3 HS/1 LS (top) and in the 1 HS/3 LS states (bottom).[54]

magnetic switching behavior can be characterized in solution (by ^{1}H NMR and UV/Vis spectroscopy) and in the solid state (by X-ray structure analysis, magnetic susceptibility measurements, and Mössbauer spectroscopy). Very gradual and incomplete transitions without hysteresis seem to be typical for all investigated, magnetically active [2×2] Fe_4^{II} arrays. Intramolecular cooperativity between the four iron centers was revealed, and improving the intermolecular interaction between the tetranuclear centers by introduction of hydrogen bonding between the grid units increased the HS fraction over the whole temperature range, although the spin transition remained very gradual and incomplete.[54]

In a farther-reaching perspective, molecular architectures such as $[Fe_4^{II}(\mathbf{5a})_4]^{8+}$ present spin state properties that may be switched by external triggers, and may provide access to (supra)molecular spintronic devices.

5.1.4. Optical States

The UV/Vis spectra of the [2×2] metal ion arrays $[Co_4^{II}(\mathbf{15a})_4]^{8+}$ and $[Co_4^{II}(\mathbf{15b})_4]^{8+}$ both bearing acidic protons display reversible pH-modulation of the optical properties in

solution. Due to the high accumulated charge of the complex cations, the eight N–H protons of the bis(hydrazone) ligands **15** ($R^1 = Ph$; see Figure 6) can be abstracted progressively and reversibly at relatively low pH values (below 7).[24a] The color of the solution of $[Co_4^{II}(\mathbf{15a})_4]^{8+}$ ($R^2 = H$, $R^3 = H$) changes from pale-yellow at low pH to orange and finally to deep violet above neutral pH, and repeated cycling indicates that the process is completely reversible (Figure 24).

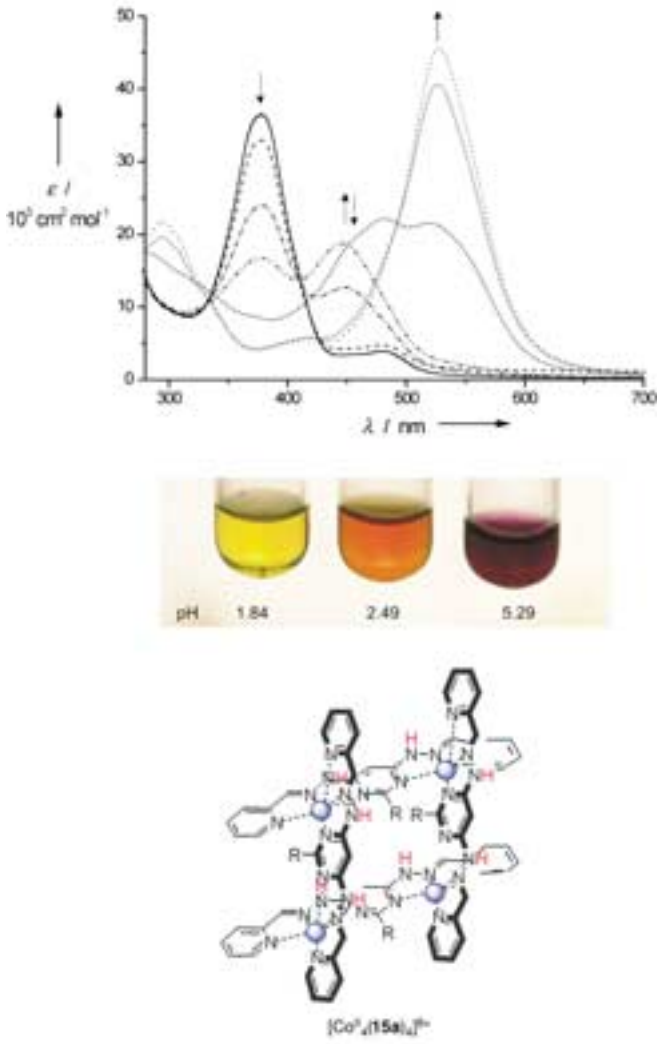

Figure 24. The color change and UV/Vis spectra of complex $[Co_4^{II}(\mathbf{15a})_4](BF_4)_8$ ($R^1 = Ph$; the abstracted acidic protons are labeled in red) depending on the pH of the acetonitrile/water solution.[24a]

Furthermore, the $[Zn_4^{II}(\mathbf{15a})_4]^{8+}$ ($R^1 = Ph$; $R^2 = R^3 = H$) complex exhibits an emission (originating from sandwich-like π–π interactions of the phenyl substituents intercalated between two ligands **15a**), which depends on the protonation state.[55]

5.2. Two-Dimensional Ordering and Addressability
5.2.1. Two-Dimensional Self-Ordering in Crystals

Simple mononuclear metal complexes bearing H-bonding-donor and -acceptor sites are able to undergo hierarchical self-assembly processes. The same approach can also be applied to [2 × 2] grids, which can be organized into a chessboard-like 2D "grid-of-grids" arrangement (Figure 25). This strategy is a powerful alternative to the more laborious stepwise construction of high nuclearity metalloarrays.

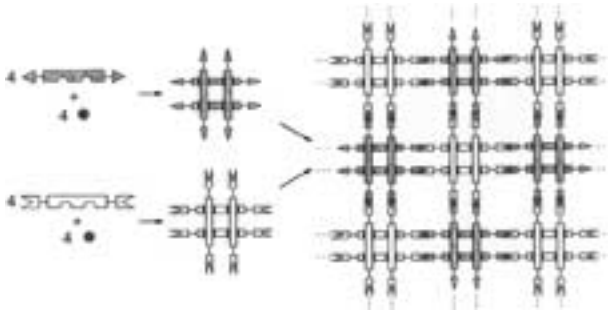

Figure 25. Schematic representation of the two-step hierarchical self-assembly sequence to generate a 2D "grid-of-grids" pattern.

Such 2D-extended supramolecular arrays of precise architecture would be of special interest for addressing the metal ions individually. However, their formation and stabilization requires control over the various noncovalent interactions, so as to make them the thermodynamically preferred products and to avoid clusterlike structures as result of undesired interactions. The hierarchical self-organization of mononuclear metal complexes with the ligands **17** or **18**, which form self-complementary hydrogen bonds, illustrates the problems. Since the energies for the formation of the double hydrogen bonds are almost the same order of magnitude as the energies of crystal packing phenomena and π–π interactions, different thermodynamic products could be observed in these experiments.

The self-complementary aminopyrimidine units of the monotopic terpyridine-type ligand **17** lead to an infinite two-dimensional gridlike structure of the corresponding $[Co^{II}(\mathbf{17})_2](PF_6)_2$ in the solid state.[56] The complexes are connected by intermolecular double hydrogen-bonds between the amino groups and the noncoordinating pyrimidine nitrogen atoms. This creates a sinusoidal arrangement of the complexes, which are interwoven into a two-dimensional network (Figure 26). However, changing the counteranion from PF_6^- to BF_4^- causes a partial breakup of this grid motif leaving one quarter of the H-bonding sites unsaturated.

The extension of this methodology towards [2 × 2] gridlike complexes afforded 2D arrays representing dual levels of organization. The complex $[Co_4^{II}(\mathbf{19})_4](BF_4)_8$ was characterized by single-crystal X-ray diffraction.[57] Although the presence of the aminopyrimidine units in the ligand should enable their metal complexes to generate hydrogen-bonded networks of grids, the hydrogen-bonding motif is only present

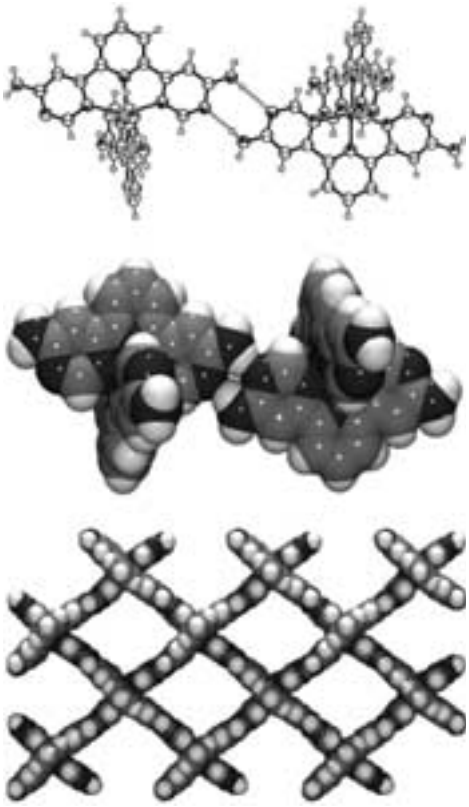

Figure 26. X-ray structure analysis of the mononuclear complex $[Co^{II}(\mathbf{17})_2](PF_6)_2$. The complex ions are arranged to give sinusoidal arrangements through the formation of double hydrogen-bonds. Top: Section with two complex ions with hydrogen boding contacts (ORTEP representation); middle: space-filling representation. Bottom: Infinite 2D gridlike metal ion array extracted from the crystal packing diagram.[56]

in one dimension, leading to the formation of infinite one-dimensional chains of grids. Neighboring complexes without hydrogen-bonding interactions show weak π-stacking between their ligands. Thus, $[Co^{II}_4(\mathbf{20})_4](BF_4)_8$ only generates a partially hydrogen-bonded network, because of the competition between hydrogen bonding and π–π stacking interactions.

The different structural outcomes of the mono- as well as the tetranuclear H-bonding approach illustrate the subtle energy interplay between H-bonding and crystal packing effects. This exemplifies a general problem found for this type of hierarchical self-assembly process.

5.2.3. *Two-Dimensional Ordering at Surfaces and Single Molecule Addressing*

One important factor in the exploitation of supramolecular architectures as components of functional devices is the ability to prepare ordered structures on solid surfaces. Recent advances in scanning probe techniques (STM, AFM) have enabled imaging and manipulation of surface-bound objects with molecular resolution.[58] Thin films of metalloorganic grid complexes have been studied by these methods with the prospect that the resulting high density of active elements could be engineered into functional surfaces, for example, memory devices.

Highly stable monolayers of the cobalt(II) [2 × 2] complex $[Co^{II}_4(\mathbf{5a})_4]^{8+}$ were prepared on an atomically flat graphite surface (highly ordered pyrolytic graphite (HOPG)) by evaporation of dilute acetone solutions, yielding defect-free areas of up to 0.5 μm^2.[59] The ordered structures form spontaneously, growing outward from single nucleation points; this process may be viewed as a two-dimensional crystallization. It was found that the orientation of the grids relative to the surface plane is controlled by the substitution pattern of ligand **5a**: the ligand with $R^1,R^2 = H$ and $R^3 = CH_3$ gave an edgewise orientation of grids with respect to the surface, while the ligand with $R^1 = CH_3$ and $R^2,R^3 = H$ resulted in flat tiles forming a superarray of [2 × 2] metallogrids. The superarray arrangement was reflected in an orthogonal 2.5 nm × 2.4 nm periodicity in the STM image (Figure 27a).

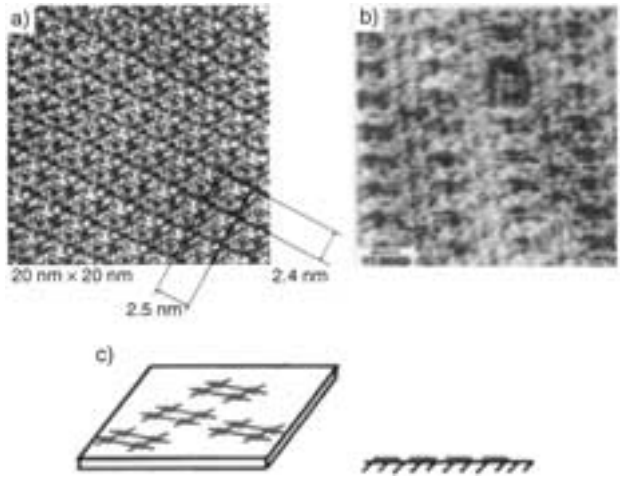

Figure 27. a) STM image of the monolayer of $[Co^{II}_4(\mathbf{5a})_4]^{8+}$ gridlike compounds on graphite. b) Hole in the monolayer produced by potential-induced lifting of a single $[Co^{II}_4(\mathbf{5a})_4]^{8+}$ molecule with the STM tip. c) Schematic representation of the disposition of the metalloarrays at the surface (top and side view).[59]

A −500 mV voltage pulse applied to the STM tip (normally operated at below −50 mV for imaging) was employed to pluck a single grid from the monolayer, resulting in a square hole with the dimensions of a single gridlike complex (Figure 27b). This represents the first indication for the possibility of controlled addressing of the [2 × 2] metalloarrays using state-of-the-art technological devices. The migration rate of the hole was measured, and found to be 200 times slower than for a monolayer of cycloalkanes, reflecting strong adsorption to the graphite surface.[60]

Analogous [2 × 2] gridlike Co^{II} complexes formed by bis(terpyridine)-derived ligands substituted with an additional *para*-pyridyl or n-propyl thia unit **5a** were adsorbed as monolayers on graphite (HOPG). They gave rise to a weaker adsorption and higher mobility compared to the corresponding parent complex.[61,62]

Thin films of [2 × 2] Co^{II}_4 metallogrids on gold surfaces have been prepared and imaged by in situ electrochemical deposition STM. Films of pure cobalt grid are poorly conductive ($< 10^{-6}$ S cm^{-1}), but upon doping with an excess of cadmium(II) ions, conductivity rises by four orders of magnitude to 10^{-2} S cm^{-1} resulting from additional electronic states in the material's insulating bandgap. While this increase is large, conductivity is still low relative to metallic conductors such as copper (10^{6}–10^{8} S cm^{-1}).[63] [2 × 2] Co^{II}_4 grid complexes have been included in thin films[64a] and may serve as components[64b] for metallosupramolecular polymers providing novel properties to the polymeric network.[64c] Recently, a Mn^{II}_9 grid (derived from a ligand similar to **13**; Figure 6) was similarly investigated on a Au(111) surface.[65]

A two-step process of an air–water interfacial reaction between free ligand **1a** (R = Ph) and Ag^{I} ions contained in the aqueous subphase led to the formation of a [2 × 2] Ag^{I}_4 grid complex, followed by its self-assembly into an oriented crystalline monolayer. On surface compression, the original monolayer underwent a transition to a crystalline bilayer, almost retaining the initial in-plane arrangement.[66]

A single report of thin film preparation employing grids of higher order concerns the silver(I) [3 × 3] complex $[Ag_9(\mathbf{1b})_6]^{9+}$. Self-assembly of the grids was achieved at the air–water interface by spreading uncomplexed ligand **1b** on an aqueous solution of silver(I) triflate. This gave ordered crystalline films of 13–20 Å thickness that could be transferred successfully onto quartz slides.[67] Grazing incidence X-ray diffraction (GIXD) revealed that grid orientation in the films could be controlled by varying the substituents of ligand **1b**: the grids lie parallel to the surface when R = Ph, but "stand up" normal to the air–water interface when R = CH_3. Thus, the formation of metallogrid monolayers represents a twofold self-assembly sequence; conventional synthetic techniques are only employed for preparation of the ligand.

6. Conclusion and Outlook

The synthetic accessibility by self-assembly of two-dimensionally arrayed switchable elements of nanometric size complements theoretical developments in molecular information storage and processing.[1,2] Gridlike metal ion architectures are attractive in this context for several reasons. For example, grid-type arrays can behave as multilevel electronic species, triggered by electrochemical, magnetic, and optical parameters. In addition, it has been shown that single grid units on surfaces are addressable within the nanometer regime. It is important to recognize the challenges that remain in order to combine these two main features in a working functional device by detecting, controlling, and addressing the electronic or magnetic states of individual grids or even ions, for instance in 2D monolayers. The information-representing metastable states must be sufficiently robust to permit room-temperature operation. The question of implementation and integration of possible devices with the supporting frame (wiring, pinning, powering) has yet to be addressed.

A sense for the potential of information storage using (supra)molecular memory elements can be obtained by contrasting the density of magnetic disk and CD-ROM technologies (~10^{8} bits cm^{-2}) with the estimated storage capacity of DNA (10^{21} bits cm^{-3} corresponding to ~10^{10} bits cm^{-2}). The cationic metalloarrays, deposited on surfaces, have shown external dimensions in the order of 25 × 25 Å and a closely packed 2D array; with one data bit stored per [2 × 2] matrix, they would lead to a potential surface data storage density of about 10^{12} bits cm^{-2}.

Gridlike arrays display "ion dot" type features, by analogy with semiconductor quantum dot arrays.[3a] One may remark that "ion dots" are of much smaller size than quantum dots. It has been pointed out that "… such architectures may foreshadow multistate digital supramolecular chips for information storage in and retrieval from inscribed patterns that might be addressable by light or electrically. Different states could, in principle, be characterized either by different local features at a given *x*, *y* coordinate, in ion dot fashion, or by specific overall optical or oxidation levels. Inducing ± 1 redox changes at specific locations in a single unit would then correspond to a sort of single electronics at ion dots."[3a]

In conclusion, the power of self-assembly to create ordered nanostructures of intriguing technological potential has been underlined through the investigation of metalloorganic grid complexes. It has been stressed that self-organization represents a self-fabrication process, allowing in principle one to bypass tedious nanofabrication procedures.[3] Considering the panoramic properties of transition-metal compounds, and the small collection of metals and ligands that have as yet been incorporated into metallogrid or other types of architectures, there can be little doubt that a very wide set of nanosize devices and materials with a rich palette of properties will spring from novel metal–ligand combinations for the benefit of the development of supramolecular electronics, spintronics, and optotronics.[68]

The authors are very thankful to Prof. M. Krische and Dr. E. Archer, University of Texas, Austin, for initiating and stimulating the writing of this review article as well as to all the other coworkers in our group who have contributed to the work reviewed herein: Dr. C. Arana, Dr. D. M. Bassani, Dr. P. N. W. Baxter, Dr. M. Barbiou, G. Blasen, Dr. E. Breuning, Prof. K. Fromm, Dr. A. Garcia, Prof. G. Hanan, Dr. A. Marquis, Dr. V. Patrowiak, Prof. U. S. Schubert, Dr. D. Volkmer, Dr. U. Ziener. We also acknowledge very fruitful collaborations with several laboratories on different aspects of the work, as indicated by the references cited.

Received: October 16, 2003 [A636]
Published Online: June 9, 2004

[1] a) M. C. Petty, M. R. Bryce, D. Bloor, *Introduction to Molecular Electronics*, Oxford University Press, New York, **1995**; b) J. M. Tour, *Acc. Chem. Res.* **2000**, *33*, 791–804; c) A. R. Pease, J. O. Jeppesen, J. F. Stoddart, Y. Luo, C. P. Collier, J. R. Heath, *Acc. Chem. Res.* **2001**, *34*, 433–444.

[2] C. Joachim, J. K. Gimzewski, A. Aviram, *Nature* **2000**, *408*, 541–548; R. F. Service, *Science* **2001**, *293*, 782–785.

[3] a) J.-M. Lehn, *Supramolecular Chemistry. Concepts and Perspectives*, VCH, Weinheim, **1995**, chap. 9, p. 200; b) J.-M. Lehn, *Science* **2002**, *295*, 2400 – 2403; J.-M. Lehn, *Proc. Natl. Acad. Sci. USA* **2002**, *99*, 4763 – 4768.

[4] a) J. Rojo, F. J. Romero-Salguero, J.-M. Lehn, G. Baum, D. Fenske, *Eur. J. Inorg. Chem.* **1999**, 1421 – 1428; b) V. Patroniak, P. N. W. Baxter, J.-M. Lehn, M. Kubicki, M. Nissinen, K. Rissanen, *Eur. J. Inorg. Chem.* **2003**, 4001 – 4009.

[5] a) L. Zhao, Z. Xu, L. K. Thompson, S. L. Heath, D. O. Miller. M. Ohba, *Angew. Chem.* **2000**, *112*, 3244 – 3247; *Angew. Chem. Int. Ed.* **2000**, *39*, 3114 – 3117; b) L. K. Thompson, L. Zhao, Z. Xu, D. O. Miller, W. M. Reiff, *Inorg. Chem.* **2003**, *42*, 128 – 139.

[6] M. Barbiou, J.-M. Lehn, *J. Am. Chem. Soc.* **2003**, *125*, 10257 – 10265.

[7] a) S. Williams, www.nanotechweb.org/articles/news/1/9/8/1 **2002**; b) R. F. Service, *Science* **2003**, *302*, 556 – 558; c) Z. Zhong, D. Wang, Y. Cui, M. W. Bockrath, C. M. Lieber, *Science* **2003**, *302*, 1377 – 1380.

[8] C. S. Lent, B. Isaksen, M. Lieberman, *J. Am. Chem. Soc.* **2003**, *125*, 1056 – 1063; M. Lieberman, S. Chellamma, B. Varughese, Y. Wang, C. Lent, G. H. Bernstein, G. Snider, F. C. Peiris, *Ann. N. Y. Acad. Sci.* **2002**, *960*, 225 – 239; A. O. Orlov, I. Amlani, G. H. Bernstein, C. S. Lent, G. L. Snider, *Science* **1997**, *277*, 928 – 930.

[9] C. S. Lent, P. D. Tougaw, *Proc. IEEE* **1997**, *85*, 541.

[10] P. J. Stang, B. Olenyuk, *Acc. Chem. Res.* **1997**, *30*, 502 – 518; D. L. Caulder, K. N. Raymond, *Acc. Chem. Res.* **1999**, *32*, 975 – 982; J.-M. Lehn in *Supramolecular Science: Where It Is and Where It Is Going* (Eds.: R. Ungaro, E. Dalcanale), Kluwer, Amsterdam, **1999**; G. F. Swiegers, T. J. Malefetse, *Chem. Rev.* **2000**, *100*, 3483 – 3537.

[11] P. N. W. Baxter in *Comprehensive Supramolecular Chemistry, Vol. 9* (Eds.: J.-M. Lehn, J. L. Atwood, J. E. D. Davies, D. D. MacNicol, F. Vögtle), Pergamon, Oxford, **1996**, pp. 254 – 288; G. S. Hanan, D. Volkmer, U. S. Schubert, J.-M. Lehn, G. Baum, D. Fenske, *Angew. Chem.* **1997**, *109*, 1929 – 1931; *Angew. Chem. Int. Ed. Engl.* **1997**, *36*, 1842 – 1844.

[12] A. W. Maverick, F. E. Klavetter, *Inorg. Chem.* **1984**, *23*, 4129 – 4135; R. Köhler, B. Kirmse, R. Richter, J. Sieler, E. Hoyer, L. Beyer, Z. *Anorg. Allg. Chem.* **1986**, *537*, 133 – 144.

[13] a) M. T. Youinou, N. Rahmouni, J. Fischer, J. A. Osborn, *Angew. Chem.* **1992**, *104*, 771 – 773; *Angew. Chem. Int. Ed. Engl.* **1992**, *31*, 733 – 735; b) P. N. W. Baxter, J.-M. Lehn, B. O. Kneisel, D. Fenske, *Chem. Commun.* **1997**, 2231 – 2232.

[14] S. Toyota, C. R. Woods, M. Benaglia, R. Haldimann, K. Wärnmark, K. Hardcastle, J. S. Siegel, *Angew. Chem.* **2001**, *113*, 773 – 776; *Angew. Chem. Int. Ed.* **2001**, *40*, 751 – 754.

[15] P. van Koningsbruggen, E. Müller, J. G. Haasnoot, J. Reedijk, *Inorg. Chim. Acta* **1993**, *208*, 37 – 42.

[16] G. S. Hanan, PhD thesis, Université Louis Pasteur, Strasbourg, **1995**.

[17] A. M. Garcia, F. J. Romero-Salguero, D. Bassani, J.-M. Lehn, G. Baum, D. Fenske, *Chem. Eur. J.* **1999**, *5*, 1803 – 1808.

[18] J. C. Jeffery, P. L. Jones, K. L. V. Mann, E. Psillakis, J. A. McCleverty, M. D. Ward, C. M. White, *Chem. Commun.* **1997**, 175 – 176.

[19] M. Ruben, J.-M. Lehn, unpublished results.

[20] J. Rojo, J.-M. Lehn, G. Baum, D. Fenske, O. Waldmann, P. Müller, *Eur. J. Inorg. Chem.* **1999**, 517 – 522.

[21] a) C. J. Mathews, K. Avery, Z. Xu, K. L. Thompson, L. Zhao, D. O. Miller, K. Biradha, K. Poirier, M. J. Zaworotko, C. Wilson, A. E. Goeta, J. A. K. Howard, *Inorg. Chem.* **1999**, *38*, 5266 – 5281; b) L. Zhao, C. J. Matthews, L. K. Thompson, S. L. Heath, *Chem. Commun.* **2000**, 265 – 266; c) L. Zhao, Z. Xu, L. K. Thompson, D. O. Miller, *Polyhedron* **2001**, *20*, 1359 – 1364.

[22] a) C. Duan, Z. Liu, X. You, F. Xue, T. C. W. Mak, *Chem. Commun.* **1997**, 381 – 382; b) A. Gelasco, A. Askenas, V. L. Pecoraro, *Inorg. Chem.* **1996**, *35*, 1419 – 1420.

[23] Efficient synthesis of **15a** and **15b** by hydrazone formation: K. M. Gardiner, R. G. Khoury, J.-M. Lehn, *Chem. Eur. J.* **2000**, *6*, 4124 – 4131; J.-L. Schmitt, A.-M. Stadler, N. Kyritsakas, J.-M. Lehn, *Helv. Chim. Acta* **2003**, *86*, 1598 – 1624.

[24] a) M. Ruben, J.-M. Lehn, G. Vaughan, *Chem. Commun.* **2003**, 1338 – 1339; b) L. H. Uppadine, J.-M. Lehn, *Angew. Chem.* **2004**, *116*, 242 – 245; *Angew. Chem. Int. Ed.* **2004**, *43*, 240 – 243.

[25] J. Hausmann, G. B. Jameson, S. Brooker, *Chem. Commun.* **2003**, 2992 – 2993; D. S. Cati, J. Ribas, J. Ribas-Ariño, H. Stoeckli-Evans, *Inorg. Chem.* **2004**, 43, 1021 – 1030.

[26] a) D. M. Bassani, J.-M. Lehn, K. Fromm, D. Fenske, *Angew. Chem.* **1998**, *110*, 2534 – 2537; *Angew. Chem. Int. Ed.* **1998**, *37*, 2364 – 2367; b) S. T. Howard, *J. Am. Chem. Soc.* **1996**, *118*, 10269 – 10274; c) D. M. Bassani, J.-M. Lehn, G. Baum, D. Fenske, *Angew. Chem.* **1997**, *109*, 1931 – 1933; *Angew. Chem. Int. Ed. Engl.* **1997**, *36*, 1845 – 1848; D. M. Bassani, J.-M. Lehn, *Bull. Soc. Chim. Fr.* **1997**, *134*, 897 – 906; M. Okhita, J.-M. Lehn, G. Baum, D. Fenske, *Chem. Eur. J.* **1999**, *5*, 3471 – 3478.

[27] R. Krämer, J.-M. Lehn, A. Marquis-Rigault, *Proc. Natl. Acad. Sci. USA* **1993**, *90*, 5394 – 5398.

[28] T. Bark, M. Düggeli, H. Stoeckli-Evans, A. von Zelevsky, *Angew. Chem.* **2001**, *113*, 2924 – 2927; *Angew. Chem. Int. Ed.* **2001**, *40*, 2848 – 2850.

[29] P. N. W. Baxter, J.-M. Lehn, J. Fischer, M.-T. Youinou, *Angew. Chem.* **1994**, *106*, 2432 – 2434; *Angew. Chem. Int. Ed. Engl.* **1994**, *33*, 2284 – 2287.

[30] a) E. Breuning, G. S. Hanan, F. J. Romero-Salguero, A. M. García, P. N. W. Baxter, J.-M. Lehn, E. Wegelius, K. Rissanen, H. Nierengarten, A. van Dorsselaer, *Chem. Eur. J.* **2002**, *8*, 3458 – 3466; b) H. Nierengarten, E. Leize, E. Breuning, A. García, F. Romero-Salguero, J. Rojo, J.-M. Lehn, A. van Dorsselaer, *J. Mass Spectrom.* **2002**, *37*, 56 – 62; c) G. S. Hanan, C. R. Arana, J.-M. Lehn, G. Baum, D. Fenske, *Chem. Eur. J.* **1996**, *2*, 1292 – 1299.

[31] a) P. N. W. Baxter, J.-M. Lehn, G. Baum, D. Fenske, *Angew. Chem.* **1997**, *109*, 2067 – 2070; *Angew. Chem. Int. Ed. Engl.* **1997**, *36*, 1978 – 1981; b) M. Schmittel, V. Kalsani, D. Fenske, A. Wiegrefe, *Chem. Commun.* **2004**, 490 – 491.

[32] L. K. Thompson, C. J. Matthews, L. Zhao, Z. Xu, D. O. Miller, C. Wilson, M. A. Leech, J. A. K. Howard, S. L. Heath, A. G. Whittaker, R. E. P. Winpenny, *J. Solid State Chem.* **2001**, *159*, 308 – 320.

[33] P. N. W. Baxter, J.-M. Lehn, G. Baum, D. Fenske, *Chem. Eur. J.* **2000**, *6*, 4510 – 4517.

[34] a) C. J. Matthews, S. T. Onions, G. Morata, M. Bosch Salvia, M. R. J. Elsegood, D. J. Price, *Chem. Commun.* **2003**, 320 – 321; b) S. T. Onions, A. M. Frankin, P. N. Horton, M. B. Hursthouse, C. J. Matthews, *Chem. Commun.* **2003**, 2864 – 2865; c) Z. He, C. He, Z.-M. Wang, E.-Q. Gao, Y. Lin, C.-H. Yan, *J. Chem. Soc. Dalton Trans.* **2004**, *502*–504.

[35] P. N. W. Baxter, J.-M. Lehn, K. Rissanen, *Chem. Commun.* **1997**, 1323 – 1324.

[36] A. Marquis, J.-P. Kintzinger, R. Graff, P. N. W. Baxter, J.-M. Lehn, *Angew. Chem.* **2002**, *114*, 2884 – 2888; *Angew. Chem. Int. Ed.* **2002**, *41*, 2760 – 2764; Erratum: A. Marquis, J.-P. Kintzinger, R. Graff, P. N. W. Baxter, J.-M. Lehn, *Angew. Chem.* **2002**, *114*, 3888; *Angew. Chem. Int. Ed.* **2002**, *41*, 3738.

[37] B. Hasenknopf, J.-M. Lehn, B. O. Kneisel, G. Baum, D. Fenske, *Angew. Chem.* **1996**, *108*, 1987 – 1990; *Angew. Chem. Int. Ed. Engl.* **1996**, *35*, 1838 – 1840; B. Hasenknopf, J.-M. Lehn, N. Boumediene, A. Dupont-Gervais, A. van Dorsselaer, B. O. Kneisel, D. Fenske, *J. Am. Chem. Soc.* **1997**, *119*, 10956 – 10958.

[38] a) C. S. Campos-Fernández, R. Clérac, K. R. Dunbar, *Angew. Chem.* **1999**, *111*, 3685 – 3688; *Angew. Chem. Int. Ed. Engl.* **1999**, *38*, 3477 – 3479; b) X.-H. Bu, H. Morishita, K. Tanaka, K. Biradha, S. Furusho, M. Shionoya, *Chem. Commun.* **2000**, 971 – 972.

[39] C. S. Campos-Fernández, R. Clérac, J. M. Koomen, D. H. Russell, K. R. Dunbar, *J. Am. Chem. Soc.* **2001**, *123*, 773 – 774.
[40] P. N. W. Baxter, R. G. Khoury, J.-M. Lehn, G. Baum, D. Fenske, *Chem. Eur. J.* **2000**, *6*, 4140 – 4145.
[41] a) M. Ruben, E. Breuning, J.-P. Gisselbrecht, J.-M. Lehn, *Angew. Chem.* **2000**, *112*, 4312 – 4315; *Angew. Chem. Int. Ed.* **2000**, *39*, 4139 – 4142; b) M. Ruben, E. Breuning, M. Barboiu, J.-P. Gisselbrecht, J.-M. Lehn, *Chem. Eur. J.* **2003**, *9*, 291 – 299; D. M. Bassani, J.-M. Lehn, S. Serroni, F. Puntoriero, S. Campagna, *Chem. Eur. J.* **2003**, *9*, 5936 – 5946.
[42] L. H. Uppadine, J.-P. Gisselbrecht, J.-M. Lehn, *Chem. Commun.* **2004**, 718 – 719.
[43] B. Barbara, L. Gunther, *Phys. World* **1999**, March, 35 – 39; C. Sangregorio, T. Ohm, C. Paulsen, R. Sessoli, D. Gatteschi, *Phys. Rev. Lett.* **1997**, *78*, 4645 – 4648.
[44] O. Kahn, *Molecular Magnetism*, VCH, Weinheim, **1993**.
[45] R. Sessoli, D. Gatteschi, A. Caneschi, M. A. Novak, *Nature* **1993**, *365*, 141 – 144; D. Gatteschi, A. Caneschi, L. Pardi, R. Sessoli, *Science* **1994**, *265*, 1054 – 1057.
[46] A.-L. Barra, P. Debranner, D. Gatteschi, R. Sessoli, *Europhys. Lett.* **1996**, *35*, 133 – 138; J. C. Goodwin, R. Sessoli, D. Gatteschi, W. Wernsdorfer, A. K. Powell, S. C. Heath, *J. Chem. Commun. Dalton Trans.* **2000**, 1835 – 1841; S. M. J. Aubin, M. W. Wemple, D. M. Adams, H.-L. Tsai, G. Christou, D. N. Hendrickson, *J. Am. Chem. Soc.* **1996**, *118*, 7746 – 7753.
[47] O. Waldmann, J. Hassmann, P. Müller, G. S. Hanan, D. Volkmer, U. S. Schubert, J.-M. Lehn, *Phys. Rev. Lett.* **1997**, *78*, 3390 – 3393; O. Waldmann, J. Hassmann, P. Müller, D. Volkmer, U. S. Schubert, J.-M. Lehn, *Phys. Rev. B* **1998**, *58*, 3277 – 3285.
[48] M. Ruben, J.-M. Lehn, V. Ksenofontov, P. Gütlich, unpublished results.
[49] Z. Xu, L. K. Thompson, D. O. Miller, *Chem. Commun.* **2001**, 1170 – 1171.
[50] a) O. Waldmann, R. Koch, S. Schromm, P. Müller, L. Zhao, L. K. Thompson, *Chem. Phys. Lett.* **2000**, *332*, 73 – 79; b) O. Waldmann, L. Zhao, L. K. Thompson, *Phys. Rev. Lett.* **2002**, *88*, 066401; c) O. Waldmann, P. Müller, M. Ruben, U. Ziener, J.-M. Lehn, *Europhys. Lett.* **2004**, submitted.
[51] O. Kahn, J. C. Martinez, *Science* **1998**, *279*, 44-48.
[52] P. Gütlich, A. Hauser, H. Spiering, *Angew. Chem.* **1994**, *106*, 2109 – 2141; *Angew. Chem. Int. Ed. Engl.* **1994**, *33*, 2024 – 2054.
[53] E. Breuning, M. Ruben, J.-M. Lehn, F. Renz, Y. Garcia, V. Ksenofontov, P. Gütlich, E. Wegelius, K. Rissanen, *Angew. Chem.* **2000**, *112*, 2563 – 2566; *Angew. Chem. Int. Ed.* **2000**, *39*, 2504 – 2507.
[54] M. Ruben, E. Breuning, J.-M. Lehn, V. Ksenofontov, F. Renz, P. Gütlich, G. Vaughan, *Chem. Eur. J.* **2003**, *9*, 4422 – 4429; corrigendum: *Chem. Eur. J.* **2003**, *9*, 5176; M. Ruben, E. Breuning, J.-M. Lehn, V. Ksenofontov, P. Gütlich, G. Vaughan, *J. Magn. Magn. Mater.* **2003**, in press.
[55] M. Ruben, M. Barbiou, J.-M. Lehn, L. Prodi, unpublished results.
[56] U. Ziener, E. Breuning, J.-M. Lehn, E. Wegelius, K. Rissanen, G. Baum, D. Fenske, G. Vaughan, *Chem. Eur. J.* **2000**, *6*, 4132 – 4139.
[57] E. Breuning, U. Ziener, J.-M. Lehn, E. Wegelius, K. Rissanen, *Eur. J. Inorg. Chem.* **2001**, 1515 – 1521.
[58] a) C. A. Mirkin, *Inorg. Chem.* **2000**, *39*, 2258 – 2272; b) J. Chen, M. A. Reed, C. L. Asplund, A. M. Cassell, M. L. Myrick, A. M. Rawlett, J. M. Tour, P. G. Van Patten, *Appl. Phys. Lett.*, **1999**, *75*, 624 – 626.
[59] A. Semenov, J. P. Spatz, M. Möller, J.-M. Lehn, B. Sell, D. Schubert, C. H. Weidl, U. S. Schubert, *Angew. Chem.* **1999**, *111*, 2701 – 2705; *Angew. Chem. Int. Ed.* **1999**, *38*, 2547 – 2550.
[60] A. Semenov, J. P. Spatz, J.-M. Lehn, C. H. Weidl, U. S. Schubert, M. Möller, *Appl. Surf. Sci.* **1999**, *144–145*, 456 – 460.
[61] U. Ziener, J.-M. Lehn, A. Mourran, M. Möller, *Chem. Eur. J.* **2002**, *8*, 951 – 957.
[62] M. Ruben, J.-M. Lehn, S. Strömsdörfer, P. Müller, unpublished results.
[63] J. Hassmann, C. Y. Hahn, O. Waldmann, E. Volz, H.-J. Schleemilch, N. Hallschmid, P. Müller, G. S. Hanan, D. Volkmer, U. S. Schubert, J.-M. Lehn, H. Mauser, A. Hirsch, T. Clark, *Mater. Res. Soc. Symp. Proc.* **1998**, *488*, 447 – 452.
[64] a) T. Salditt, Q. An, A. Blech, C. Eschbaumer, U. S. Schubert, *Chem. Commun.* **1998**, 2731 – 2732; b) U. S. Schubert, C. H. Weidl, J.-M. Lehn, *Des. Monomers Polym.* **1999**, *2*, 1 – 17; U. S. Schubert, C. Eschbaumer, *Angew. Chem.* **2002**, *114*, 3016 – 3050; *Angew. Chem. Int. Ed.* **2002**, *41*, 2892 – 2926.
[65] L. Weeks, L. K. Thompson, J. G. Shapter, K. J. Pope, Z. Xu, *J. Microsc.* **2003**, *212*, 102 – 106.
[66] I. Weissbuch, P. N. W. Baxter, I. Kuzmenko, H. Cohen, S. Cohen, K. Kjaer, P. B. Howes, J. Als-Nielsen, J.-M. Lehn, L. Leiserowitz, M. Lahav, *Chem. Eur. J.* **2000**, *6*, 725 – 734.
[67] I. Weissbuch, P. N. W. Baxter, S. Cohen, H. Cohen, K. Kjaer, P. B. Howes, J. Als-Nielsen, G. S. Hanan, U. S. Schubert, J.-M. Lehn, L. Leiserowitz, M. Lahav, *J. Am. Chem. Soc.* **1998**, *120*, 4850 – 4860.
[68] Note added in proof (April 19, 2004): Since the submission of this article, the following relevant paper has appeared: J. Nitzschke, J.-M. Lehn, *Proc. Natl. Acad. Sci. USA* **2003**, *100*, 11 970 – 11 974.

